Chapter 7
Unstable Resonators

7.1 General Aspects

If the g-parameters of the resonator mirrors fulfill the relations $g_1g_2<0$ or $g_1g_2>1$, the radiation inside the resonator cannot be characterized by a Gaussian beam. Equation (5.10) indicates that in these cases the Gaussian beam radii become complex quantities. The steady state field distributions are not given by Gauss-Hermite or Gauss-Laguerre polynomials. These resonators are referred to as *unstable resonators* [3.54,3.67], whereby the term "unstable" accounts for the fact that a Gaussian beam launched into the resonator will increase its beam radius after each round trip and, therefore, does not represent a "stable" eigensolution of the resonator (Fig. 7.1). Note that the term "unstable" does not mean that the resonator is more sensitive to mirror misalignment as compared to stable resonators. In fact, unstable resonators are generally less sensitive to mirror tilt than stable resonators in fundamental mode operation. By using the equivalent G-parameter $G=2g_1g_2-1$ we can characterize the different resonator schemes as follows:

stable resonators	:	$0 < \|G\| < 1$
resonators on the stability limits	:	$\|G\| = 1$
unstable resonators	:	$\|G\| > 1$

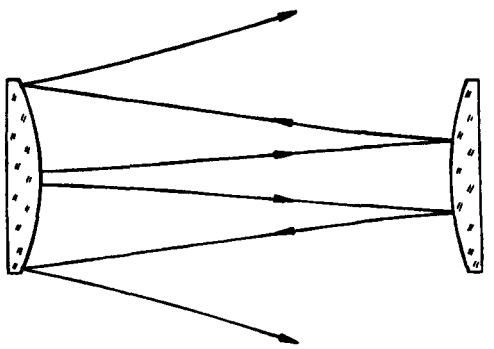

Fig. 7.1 No Gaussian beam can reproduce itself in an unstable resonator. The beam radii at the mirrors increase with each round trip.

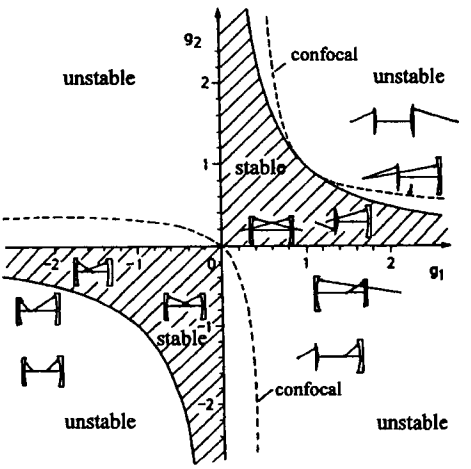

Fig. 7.2 The stability diagram of optical resonators. Unstable resonators are located in the non-hatched areas.

Furthermore, one is able to distinguish *positive branch* unstable resonators ($G>1$) and *negative branch* unstable resonators ($G<-1$). The steady state field distributions on the mirrors of unstable resonators, similar to stable resonators, are solutions of the Kirchhoff integral equation (see (5.71),(5.72)). In contrast to stable resonators, the beam propagation inside unstable resonators, to a good approximation, can be described by the propagation laws of geometrical optics. As already discussed in Sec. 1.3, unstable resonators are characterized by the presence of spherical waves whose radii of curvature reproduce themselves after each round trip. Before we investigate the mode structures and the diffraction losses by applying diffraction theory, we will discuss the basic properties of unstable resonators by analyzing the propagation of these spherical waves. Although this geometric-optical treatment does not provide information on the field distributions, the geometrical description will provide the reader with a better understanding of the basic principles of unstable resonators.

7.2Geometric Optical Description of Unstable Resonators

7.2.1 Beam Propagation

Unstable resonators are characterized by the presence of spherical waves inside the resonator that reproduce themselves after each round trip [3.54,3.55,3.67] (see Sec. 1.3). A spherical wave starting at mirror 1 with a radius of curvature R_1 is transformed by mirror 2 into a spherical wave with radius of curvature R_2 (Fig. 7.3). After hitting mirror 1 again, the initial radius of curvature R_1 is reproduced. The resonator mirrors thus image the centers of curvatures of the wave fronts Z_1 and Z_2 onto each other. In every unstable resonator we can find two spherical waves whose radii of curvature at any plane inside the resonator are

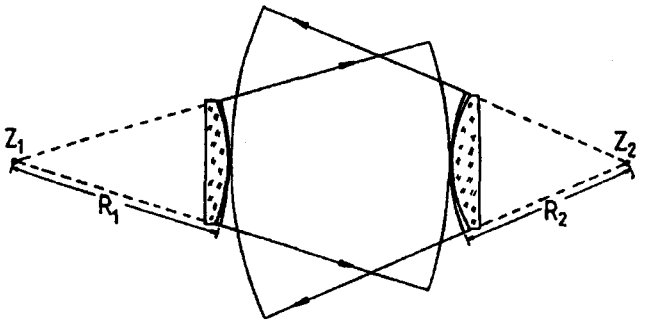

Fig. 7.3 In unstable resonators spherical waves can be found whose radii of curvatures are reproduced after each round trip. The beam propagation of the diverging wave is shown.

are reproduced after a round trip (note that in Fig. 7.3 only one spherical wave is shown!). If R_+ and R_- denote the radii of curvature at mirror 1 (after being reflected off the mirror) of the two spherical waves (Fig. 7.4), the following relation holds:

$$R_{\pm} = \frac{\pm 2Lg_2}{|G| \pm \sqrt{G^2-1} - 2g_2 + 1} \tag{7.1}$$

If mirror 1 is limited by an aperture with radius a, which means that the beam starting at mirror 1 has a diameter of $2a$, the radii of curvature R_+ and R_- reproduce themselves after the round trip, but the beam diameter is magnified by a factor M_+ and M_-, respectively, with:

$$M_{\pm} = |G| \pm \sqrt{G^2 - 1} \quad \textit{and} \quad |M_+ M_-| = 1 \tag{7.2}$$

The spherical wave with radius R_+ increases the beam radius after each round trip by the factor $|M_+|$, called the *magnification*. Since $|M_+|>1$ holds, the corresponding spherical wave is referred to as the *diverging wave*. If the power starting at mirror 1 (inside the aperture) is given by P_0, only the power

$$P_1 = \frac{1}{M_+^2} P_0 \tag{7.3}$$

hits the mirror inside the aperture after the round trip, provided that the intensity profile is homogeneous. The loss ΔV per round trip and the loss factor V per round trip are thus given by:

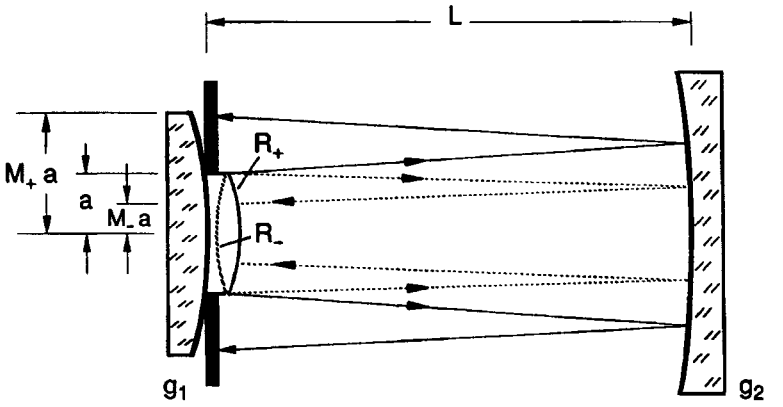

Fig. 7.4 The two self-reproducing spherical waves with radii of curvature R_+ and R_- at mirror 1 (after the reflection). After one round trip the beam diameter is changed by a factor M_+ (>1) and $|M_-|$ (M_-<1), respectively.

$$\Delta V = 1 - \frac{1}{M_+^2}, \quad V = 1 - \Delta V = \frac{1}{M_+^2} \tag{7.4}$$

The loss factor represents the power fraction that stays inside the resonator after the round trip; the remainder of the power is absorbed by or reflected off the aperture material.

In contrast to the diverging wave, the *converging wave* (R_-) decreases the beam diameter after each round trip by a factor $|M_-|$ with $|M_-|<1$. The power P_0 starting at mirror 1 is conserved, but with every round trip the beam radius at mirror 1 is continuously decreased by $|M_-|$ so that no steady state beam radius can be established on the mirror. After a few round trips in the resonator, the beam radius of the converging wave reaches its minimum value given by the diffraction limit and will then expand again. The converging wave transforms itself into a diverging wave due to diffraction. It is for this reason that the beam propagation in an unstable resonator is characterized by the divergent wave only. However, the convergent wave may have an influence on the mode properties of unstable resonators, if it is continuously excited by reflection off apertures or the endfaces of the active medium [3.67,3.125]. In the following we will deal only with the diverging wave and we will drop the index + in both the magnification and the radius of curvature for convenience.

Figure 7.5 depicts the beam propagation in an unstable resonator. Instead of limiting mirror 1 by an aperture, the size of the highly reflecting area now defines the beam size on the mirror. The laser beam is generated by output coupling around the reflective spot on the mirror. In circular symmetry, the near field exhibits the shape of an annulus with inner radius a and outer radius Ma. The size of mirror 2 is chosen such that no power is coupled out at this side of the resonator. The coatings on both mirrors are highly reflecting for the desired wavelength of laser emission.

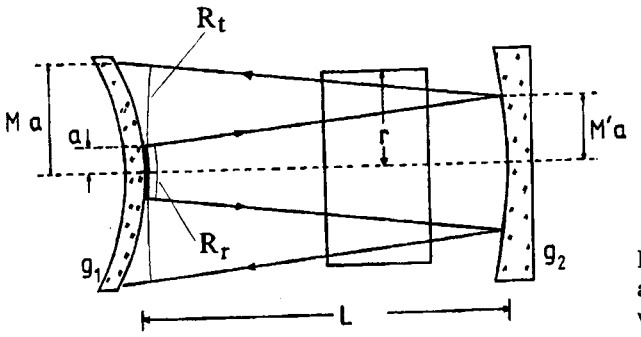

Fig. 7.5 Beam propagation inside an unstable resonator (diverging wave).

The following relations hold (see Fig. 7.5):

g-parameters: $$g_i = 1 - \frac{L}{\rho_i}, \quad i=1,2, \tag{7.5}$$

Equivalent G-parameter: $$G = 2g_1g_2 - 1 \tag{7.6}$$

Magnification (round trip): $$M = |G| + \sqrt{G^2 - 1} \tag{7.7}$$

Magnification (transit): $$M' = g_1 + \frac{\sqrt{G^2 - 1}}{2g_2} \tag{7.8}$$

Radius of curvature of the spherical wave at mirror 1:

- travelling towards the mirror: $$R_t = \frac{L}{M' + 1 - 2g_1} \tag{7.9}$$

- reflected off the mirror: $$R_r = \frac{2Lg_2}{M + 1 - 2g_2} \tag{7.10}$$

Loss factor per round trip: $$V = \frac{1}{M^2} \tag{7.11}$$

Note that in contrast to stable resonators, the loss of the resonator represents the power fraction coupled out of the resonator.

Example: $\rho_1 = -0.5m$, $\rho_2 = 2m$, $L = 0.75m$
---------> $g_1 = 2.5$, $g_2 = 0.625$, $G = 2.125$
$M = 4$, $M' = 4$, $R_t = \infty m$, $R_r = 0.25$ m
Loss factor per round trip : $V = 0.0625$

Three different ways to accomplish this special output coupling scheme in unstable resonators exist (Fig. 7.6). The high reflecting, confined mirror can be held in place by thin pins or mounted in the bore of a highly transmitting substrate (b). More common is the application of a high reflecting coating on an AR coated substrate as depicted in (a). For CO_2 lasers and other lasers emitting in the wavelength range on the order of 10μm, the output coupling by means of a scraper is a well established technique (c). The mirror is confined by an aperture (usually made of copper and polished to optical quality) that reflects the beam out of the resonator in a direction perpendicular to the optical axis of the resonator.

The loss of an unstable resonator is generated by the output coupling, which means that a higher loss might generate a higher output power. This probably sounds strange to readers that are more familiar with stable resonators, since the output power of stable resonators always decreases as the losses are increased. It takes time to adjust to the fact that the losses of unstable resonators are determined by the power fraction coupled out of the resonator and that the output coupling can be changed by varying the geometrical dimensions (mirror curvatures and length) of the resonator. It is definitely helpful to keep in mind that an unstable resonator with diffraction loss factor V per round trip provides the same output coupling as a stable resonator with a reflectivity of the output coupling mirror of $R=V$. Those readers who are not familiar with unstable resonators should therefore associate the loss factor with a mirror reflectivity.

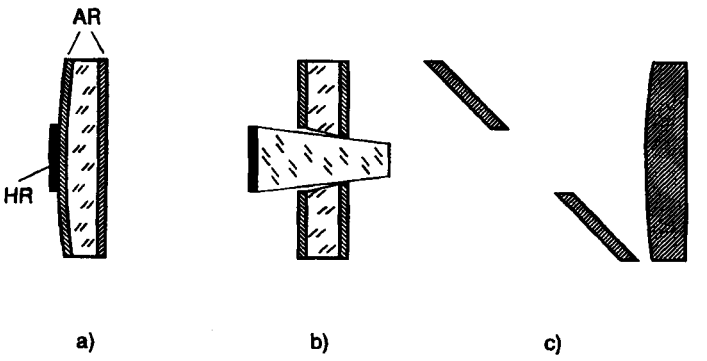

Fig. 7.6 Technical realization of the output coupling mirror of unstable resonators.

Resonator Schemes

Unstable resonators can be subdivided into two different classes:

1) $g_1g_2 > 1$, positive branch

These resonators exhibit either zero or two focal points inside the resonator. The centers of curvatures of the spherical waves at the mirrors (see Fig. 7.3) are located either outside ($g_1>0$, $g_2>0$) or inside ($g_1<0, g_2<0$) the resonator. Unstable resonators exhibiting these properties are referred to as *positive branch unstable resonators*.

2) $g_1g_2 < 0$, negative branch

One center of curvature of the spherical wave is located inside the resonator. The *negative branch unstable resonators* therefore exhibit a focal spot in the resonator. Due to possible damage of the active medium by the high intracavity intensities, these resonators are only used in high gain gas lasers. Compared to positive branch resonators they exhibit a much lower misalignment sensitivity.

Resonators for which the relation:

$$g_1 + g_2 = 2g_1g_2 \tag{7.12}$$

holds, are referred to as confocal resonators (Fig. 7.7). For confocal resonators, the focal points of the two resonator mirrors are on top of each other, which means that the unstable resonator acts like a telescope. This special mirror arrangement provides several advantages:

a) the beam radius stays constant as the beam propagates from the unconfined mirror to the output coupler (as long as diffraction is neglected). The mode volume can thus be easily adapted to the volume active medium yielding optimum fill factors.

b) the beam is coupled out in the form of a plane wave which saves transformation optics for beam handling.

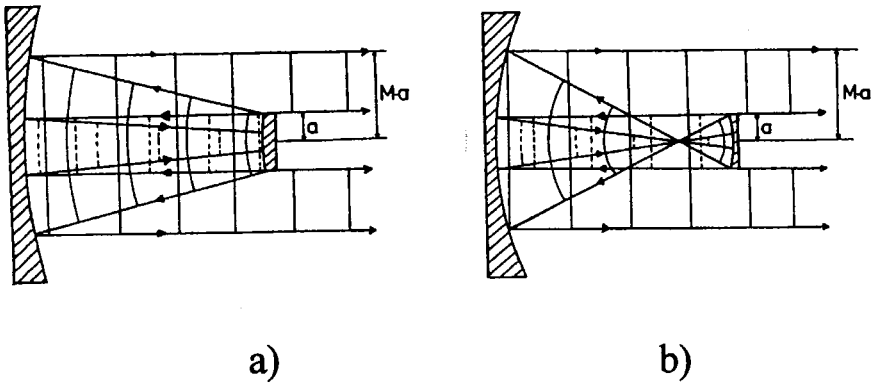

Fig. 7.7 Beam propagation in confocal unstable resonators with magnification |M|=2. a) positive branch, b) negative branch.

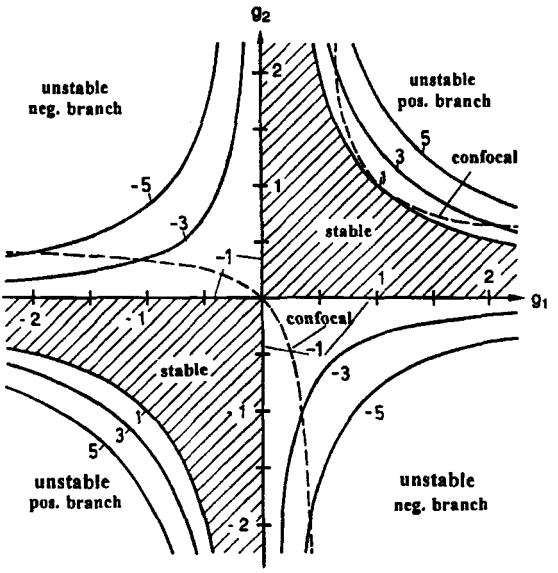

Fig. 7.8 Curves of constant magnification in the stability diagram. The broken lines indicate the confocal resonators. The curves with magnification $|M|=1$ are the stability limits.

So far the geometrical description indicates that unstable resonators having the same absolute value of the equivalent g-parameter $G=2g_1g_2-1$ exhibit the same absolute value of the magnification. Consequently, they have the same loss factor per round trip. Unstable resonators with equal losses are thus located on hyperbolas in the stability diagram, as shown in Fig. 7.8.

Unstable resonators can, of course, also be realized in rectangular symmetry. If the confined mirror has a rectangular shape and both mirrors are spherical, the beam radii in the x- and in the y-direction are both magnified by the magnification M (Fig. 7.9). The decision as to whether rectangular or circular symmetry is chosen depends on the symmetry of the active medium. In general, the resonator geometry has to be designed so that the beam travelling towards the output coupler fills the entire active medium, and optimum output coupling is provided. The geometry of the output coupler is thus determined by the geometry of the active medium. Rectangular geometry active media (slab technology) are used in CO_2 lasers and Nd:YAG lasers. The extraction of the power from the active medium is optimum for confocal resonators since the beam radius of the back travelling wave stays constant. It is for this reason that confocal positive branch unstable resonators play an important role in practical applications. The magnification is determined by the small-signal gain of the active medium. Higher gain media tolerate higher magnifications as far as the laser efficiency is concerned. Since the focusability and the misalignment sensitivity are enhanced as the magnification is increased (see later sections), unstable resonators are generally utilized in medium to high gain lasers. Typical values of the magnification are around $M=2$.

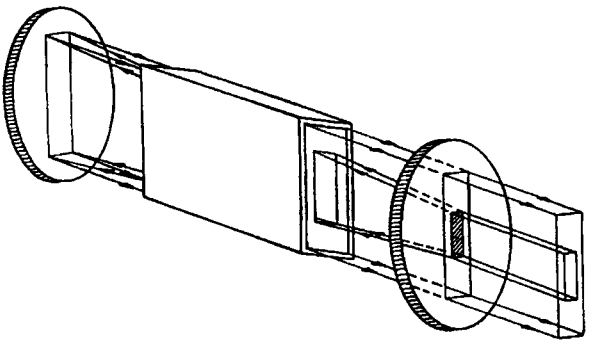

Fig. 7.9 Confocal positive branch unstable resonator in rectangular symmetry.

7.2.2 Focusability

The laser beam emerges from the unstable resonator in the form of an annular ring with inner radius a, outer radius Ma, and a radius of curvature of R_t (see (7.9)). The beam thus exhibits an angle of divergence θ_g (Fig. 7.10), with:

$$\theta_g = \frac{Ma}{R_t} \tag{7.13}$$

This angle, which can assume very high values, is generated by the geometrical set-up of the resonator (for a confocal unstable resonator $\theta_g=0$ holds), and it does not affect the beam quality of the laser. This is due to the fact that the angle of divergence can be varied by using a lens right behind the output coupler without changing the beam quality. It is advantageous to use a focal length that transforms the emerging beam into a plane wave ($\theta_g=0$), as shown in Fig. 7.11.

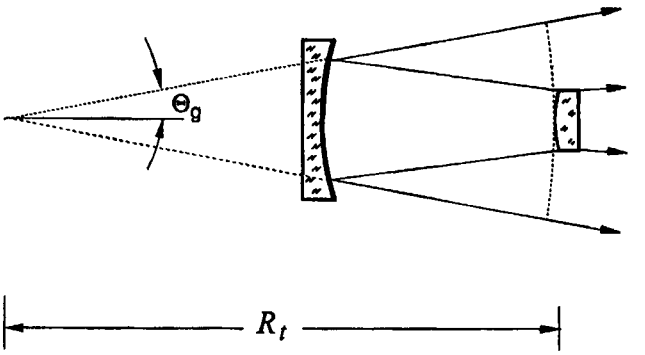

Fig. 7.10 The geometrical angle of divergence θ_g of an unstable resonator.

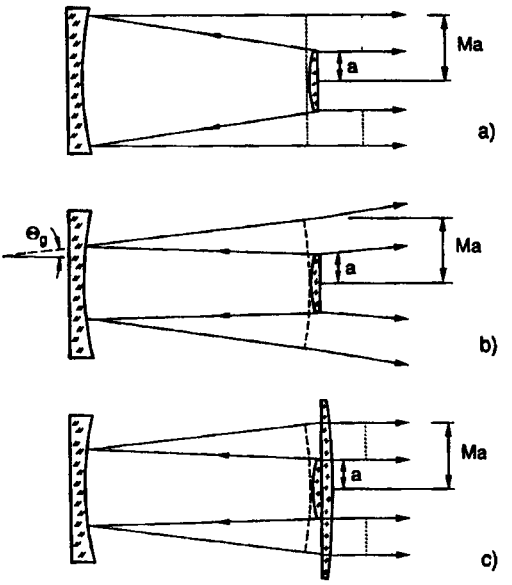

Fig. 7.11 The angle of divergence θ_g can be varied by changing the design of the resonator or by collimating the beam with a focusing lens. All three resonators shown exhibit the same beam quality. The beam quality depends on the magnification M and the mirror radius a only.

All unstable resonators having the same magnification and the same mirror radius a exhibit the same beam quality, no matter how large the geometrical angle of divergence θ_g is. The theoretical reason for this is the fact that the beam parameter product remains constant. Therefore, the beam waist w_0, which is located at the center of curvature of the spherical wave with radius R_t (virtual beam waist), is increased as the angle of divergence is decreased. The geometrical divergence angle, however, determines the position of the focus if the beam is focused by means of a lens (Fig. 7.12). Only for confocal resonators is the focal spot at the focal plane of the lens. The distance z of the focus from the lens, to a good approximation, can be calculated by using the imaging condition of geometrical optics. If x denotes the distance of the focusing lens from the output coupling mirror, the distance z reads:

$$z = \frac{f}{1 - f/(R_t + x)} \tag{7.14}$$

If w is the beam radius at the focusing lens, this relation can be written as:

$$z = \frac{f}{1 - f\theta_g/w} \tag{7.15}$$

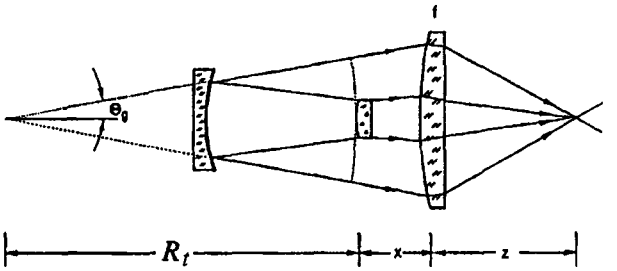

Fig. 7.12 The position of the focus of unstable resonators, to a good approximation, can be calculated by using the imaging condition of geometrical optics, as long as $w/\theta_g \ll f$.

Example: ρ_1=-0.5m, ρ_2=1.5m, L=0.7m, a=3mm, x=100mm, f=150mm (Fig. 7.12)

equivalent G-parameter	:	G	= 1.56
magnification	:	M	= 2.76
radius of curvature	:	R_t	= -2.52 m
angle of divergence	:	θ_g	= 3.28 mrad
beam radius at lens	:	w	= 8.61 mm
position of focus	:	z	= 159.1 mm

The beam quality of unstable resonators is determined by the diffraction at the confined output coupling mirror. If we assume that the outcoupled beam exhibits a plane phase front, the intensity distribution in the focal spot is given by the intensity distribution in the far field of a homogeneously illuminated annular ring with inner radius a and outer radius Ma. Application of the diffraction integral in the Fraunhofer approximation yields the far field intensity distribution:

$$I(\theta) = I(0)\,\frac{M^2}{M^2-1}\left[\frac{J_1(2\pi Ma\theta/\lambda)}{\pi Ma\theta/\lambda} - \frac{1}{M^2}\,\frac{J_1(2\pi a\theta/\lambda)}{\pi a\theta/\lambda}\right] \tag{7.16}$$

where J_1 is the Bessel function of order 1. Figure 7.13 presents far field intensity distributions calculated with (7.16) as a function of $z=2\pi Ma\theta/\lambda$. For high magnifications ($M>1$) we obtain the far field intensity distribution of a round aperture (see Sec. 2.2.2) with a full width half maximum (FWHM) diameter of the central peak of:

$$\Delta\theta = 0.51\frac{\lambda}{Ma} \tag{7.17}$$

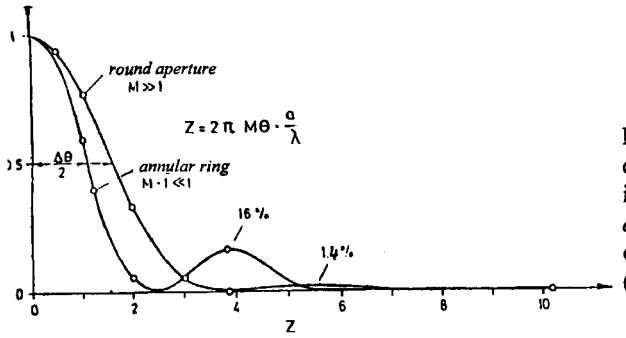

Fig. 7.13 Far field intensity distributions of a homogeneously illuminated ring with inner radius a and outer radius Ma in the limits of low and high magnification M (calculated with (7.16)).

In the limit of low magnification ($M\text{-}1 \ll 1$), we get a distribution with a narrower center peak ($\Delta\theta = 0.35\lambda/a$), but now the power fraction in the first side lobe is increased. No matter what the radius of curvature R_t of the outcoupled beam is, the intensity distribution at the focus is always given by the distribution (7.16). The radial extent of the focal spot can be calculated by using the distance z of (7.14):

$$r = z\,\Delta\theta/2 \tag{7.18}$$

The power fraction in the side lobe and the spot radius r decrease as the magnification of the resonator is increased. It is for this reason that the magnification of unstable resonators is generally chosen as high as possible with an upper limit given by the gain of the medium (a high magnification requires a high gain in order to operate the resonator at optimum output coupling). Unstable resonators are mostly applied to active media with sufficiently high small-signal gain ($g_0\ell > 1.5$). For low gain media the optimum magnification would be too low to have the major power fraction going into the central peak.

In our geometrical model, the beam waist is located at the plane of the output coupling mirror. We can thus make a first estimate of the beam parameter product by multiplying the near field diameter d_0 with 86.5% power content:

$$d_0 = 2a\sqrt{0.865M^2 + 0.135} \tag{7.19}$$

with the numerically calculated full angle of divergence Φ with 86.5% power content of the far field distribution (7.16) to get the beam parameter product:

$$\frac{d_0\Phi}{4} = \frac{a}{2}\sqrt{0.865M^2 + 0.135}\;\Phi = \frac{1}{K}\frac{\lambda}{\pi} \tag{7.20}$$

where K is the beam quality factor with $K < 1$.

Figure 7.14 shows numerically calculated beam parameter products as a function of the magnification M and the power fractions in the central peak and in the first side lobe. This graph indicates that the beam quality is enhanced as the magnification is increased. In the limit of high magnifications, the beam parameter product approaches the value for a round beam with a homogeneous intensity distribution ($K=0.375$). Compared to a Gaussian beam ($K=1$), the beam parameter product of unstable resonators is at least 2.5 times higher. For typical magnifications between $M=2$ and $M=4$, the beam quality of unstable resonators is about three times worse as compared to a Gaussian beam.

Keep in mind that the model used to calculate the beam quality assumes that the near field is a perfect annular ring. In reality the mode structure in the near field exhibits variations in both the amplitude and the phase. This diffraction effect leads to a lower power fraction in the side lobe and to slightly lower beam parameter products (see Fig. 7.14a). This is mainly due to a less steep slope in the outer area of the beam. Furthermore, with the incorporation of the mode structure the beam quality will become dependent on the mirror radius a, as will be discussed in a later section.

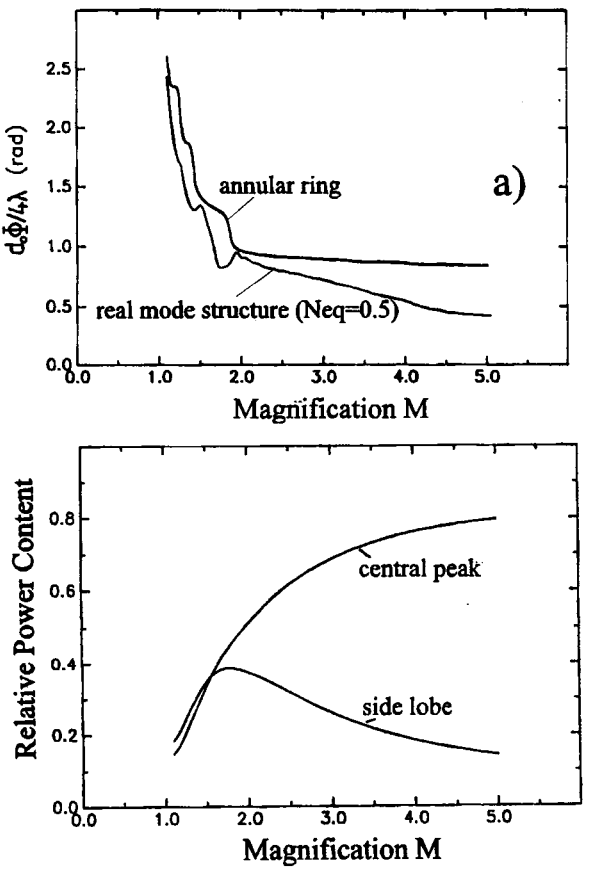

Fig. 7.14 Calculated beam parameter products (86.5% power content, upper graph) and power fractions in the center peak and in the side lobe as a function of the magnification (using the far field distribution of a homogeneously illuminated ring with inner radius a and outer radius Ma).

A similar geometrical treatment can be performed for unstable resonators in rectangular symmetry. The one-dimensional far field is given by the Fourier transform of a double slit with a slit width of *(M-1)a* and a slit separation (center-to-center) of *(M+1)a*. The angular intensity distribution in one dimension reads:

$$I(\theta) = I(0)\left[\frac{\sin[\pi\theta(M-1)a/\lambda]\ \cos[\pi\theta(M+1)a/\lambda]}{\pi\theta(M-1)a/\lambda}\right]^2 \qquad (7.21)$$

For the same magnification, the intensity distribution at the focus of unstable resonators in rectangular symmetry exhibits much higher side lobes as compared to circular symmetric unstable resonators. Figure 7.15 presents measured focal intensity distributions for both symmetries in comparison with the theoretical distributions calculated numerically with taking the near field mode structure into account. This graph clearly indicates the relation between the height of the side lobes and the magnification. Measured beam parameter products for an Nd:YAG slab laser with unstable resonators in rectangular symmetry as a function of the magnification are shown in Fig. 7.16. Similar to circular symmetry unstable resonators, the beam parameter products are 3-6 times higher as compared to a Gaussian beam.

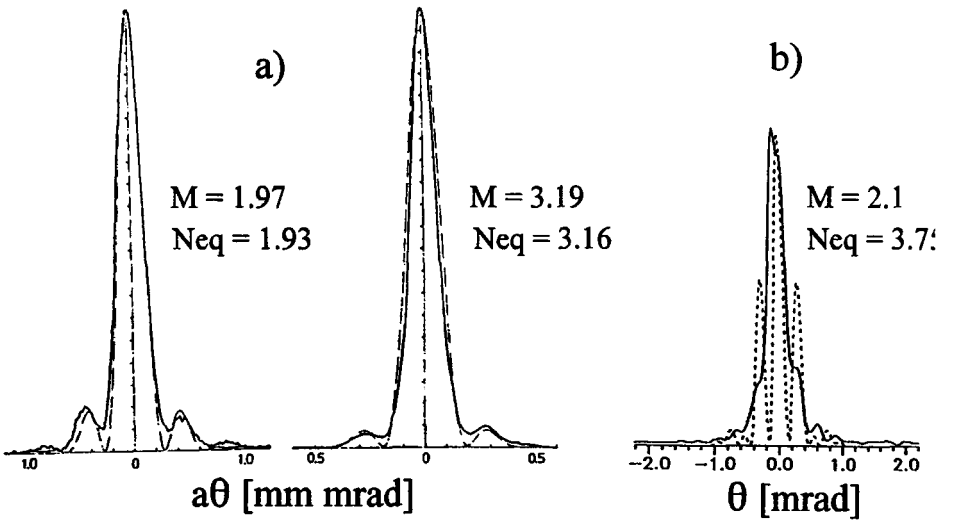

Fig. 7.15 Measured (solid lines) and calculated (broken lines) intensity distributions at the focus of unstable resonators for Nd:YAG lasers (λ=*1.064μm*). a) circular symmetry, *a=1.5mm*, b) rectangular symmetry, *a=2.0mm* [S.7].

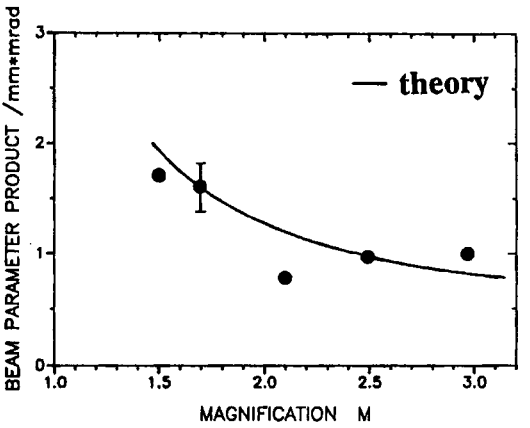

Fig. 7.16 Measured beam parameter products (86.5% power content) of an Nd:YAG slab laser (λ=1.064μm) with unstable resonators in rectangular symmetry. The beam parameter product of a Gaussian beam is 0.25mm mrad (note that this is less than λ/π due to the symmetry) [3.129] (© Chapman and Hall 1992).

It is important to understand that for unstable resonators, the intensity distribution in the far field and the intensity distribution at the focus are generally different. The two distributions are only similar if the geometrical angle of divergence θ_g is equal to zero. For a nonvanishing geometrical divergence, the far field has an annular shape whereas the intensity distribution in the focal spot is still determined by the distributions (7.16) and (7.21) and exhibits a central intensity peak. The measurement of the far field in the focal plane of a lens will thus not provide any information on the focusability of the beam. This is in contrast to stable resonator modes where identical distributions are observed in the far field and in the focus.

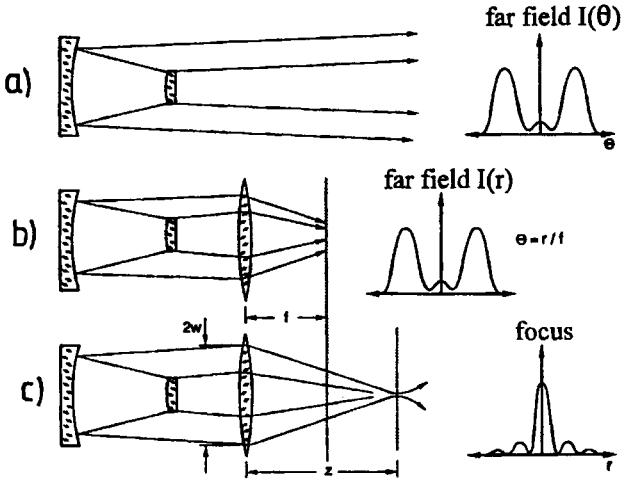

Fig. 7.17 The intensity distributions in the far field and at the focus are identical only for confocal resonators. The far field is observed in the focal plane of the lens (b) whereas the focus is found at a distance z from the lens (c).

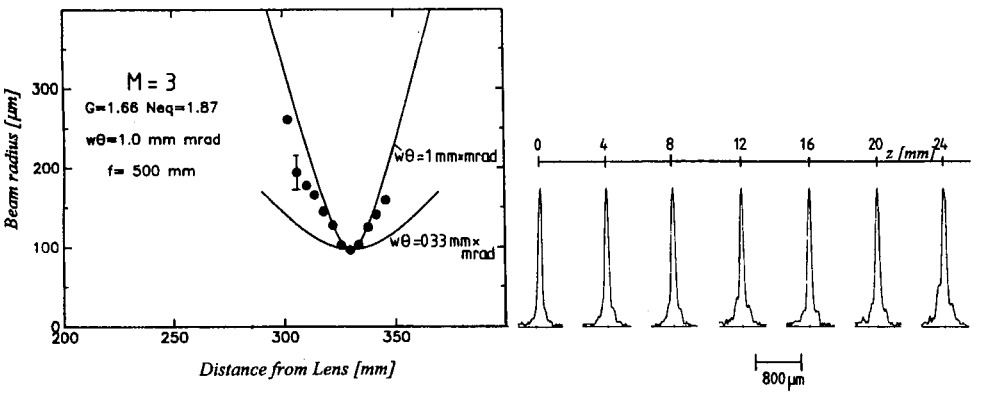

Fig. 7.18 Measured beam radii (86.5% power content) and radial intensity distributions in the vicinity of the focal spot for an unstable resonator (Nd:YAG laser, $\lambda=1.064\mu m$, $M=3$, $f=500mm$). The curves represent the caustics for a Gaussian beam (lower curve) and a higher order stable resonator mode with the same beam parameter product as that of the unstable resonator. In the right hand graph, the focus is at $z=0$.

The reason for this behavior is the fact that the mode structures of unstable resonators do not represent eigensolutions of the free space diffraction integral. This means that the mode structure changes as the beam propagates; an annular ring in the near field is transformed into a centered intensity distribution at the focus. The power fraction in the center peak is continuously transferred to the sidelobe as the observation plane is moved from the focal plane back to the output coupler. In the vicinity of the focal spot, unstable resonators thus exhibit an increase in the side lobe intensity in addition to the increase in the beam size (Fig. 7.18). This graph indicates that despite the changing intensity structure, the beam radii follow, to a good approximation, the same parabolic propagation law as a higher order stable resonator mode. The knowledge of the beam parameter product thus enables us to calculate the Rayleigh range in a way similar to stable resonators:

$$z_0 = \frac{w_0^2}{d_0\Phi/4} \tag{7.22}$$

where w_0 is the beam radius at the focus and $d_0\Phi/4$ is the beam parameter product.

So far we have assumed that the intensity distribution inside the unstable resonator is represented by a rectangular profile. Unfortunately, this is only a fair approximation of the real mode structure. Due to diffraction at the output coupler, the field distributions inside and outside the resonator exhibit a more complicated phase and amplitude structure which influence both the losses and the beam quality. The geometrical loss factor (7.11) represents

only a lower bound for the real loss factor in unstable resonators. In order to get a detailed understanding of unstable resonators the mode structure has to be calculated by using diffraction integrals. However, the geometrical discussion presented so far is not worthless, since the beam propagation can always be described by geometrical optics. Furthermore, the mode structure and the losses will converge to the geometrical quantities if the Fresnel number is chosen high enough. This is a consequence of the fact that for Fresnel numbers greater than 100, the field distributions do not change significantly during propagation and can therefore be propagated by using the laws of geometrical optics.

7.3 Diffraction Theory of Unstable Resonators

7.3.1 Mode Structures, Beam Quality, and Losses

The steady state field distributions on the mirrors of unstable resonators can be calculated similarly to those of stable resonators by applying the integral equations (5.71) in rectangular symmetry and (5.73) in circular symmetry. For both stable and unstable resonators the same integral equations can be used, the only difference is that the absolute value of the G-parameter is now greater than 1.0. Similar to the treatment of stable resonator modes, the integral equations can be simplified by separating the coordinates. The intensity distributions of the eigenmodes and the loss factor $V=|\gamma|^2$ again depend on the absolute value of the equivalent g-parameter G and the absolute value of the effective Fresnel number $N_{eff}=a^2/(2Lg_2\lambda)$. Unstable resonators exhibit an infinite set of TEM modes with mode indices $p\ell$ and mn, but the mode properties are completely different as compared to the modes of stable resonators. Figure 7.20 presents calculated loss factors per round trip of unstable resonators with magnification $M=2$ for some transverse modes in circular symmetry with $\ell=0$ and $\ell=1$. In contrast to stable resonator modes, the loss factor does not always increase as the aperture radius is increased leading to extreme values of the loss factor.

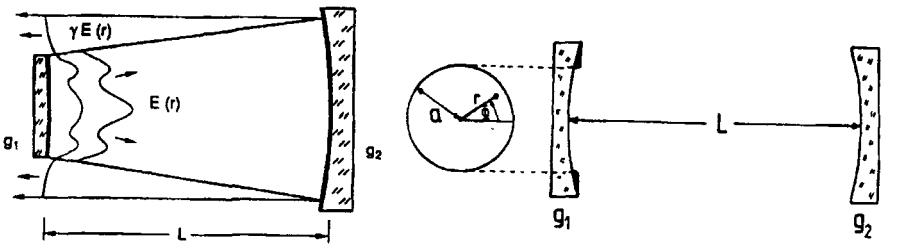

Fig. 7.19 Calculation of the field distribution at the plane of the output coupler for unstable resonators in circular symmetry. After the round trip the shape of the field at mirror 1 is still the same.

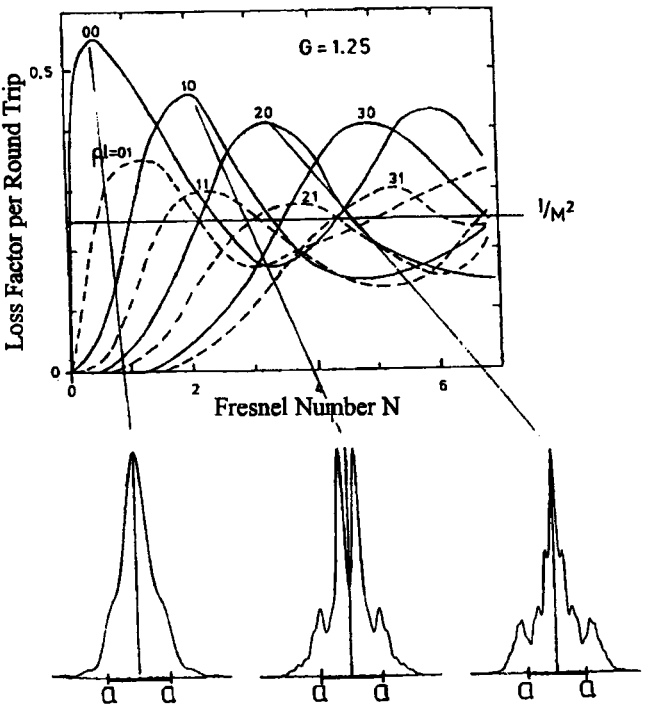

Fig. 7.20 Calculated loss factor per round trip as a function of the effective Fresnel number N for unstable resonators in circular symmetry with magnification $M=2$. The radial intensity distributions at the plane of the output coupler are shown for the first three loss factor maxima.

Since different transverse modes exhibit their maxima at different Fresnel numbers, the loss factor curves cross, which means that at this point two transverse modes have the same diffraction loss. For transverse modes without azimuthal structure ($\ell=0$) the loss factor is higher as compared to other modes and also higher than the geometrical loss factor of $1/M^2$. The reason for the lower loss becomes apparent if we investigate the intensity profiles of the modes at the loss factor maxima. Since the profiles are more centered as compared to the homogeneous profile assumed in the preceding section, a higher power fraction hits the output coupler again after the round trip resulting in a higher loss factor.

It is important to note that the beam radii of different transverse modes are the same. This property, together with the difference in diffraction loss between transverse modes, determines the special oscillation behavior of unstable resonators. The mode with the lowest loss will start oscillating first and deplete the gain in the same area of the active medium that might be used by other transverse modes. These modes, however, exhibit too high of a loss for the leftover gain to reach the laser threshold. Except for the operation at mode crossing points, unstable resonators thus oscillate in a single transverse mode with no azimuthal structure ($\ell=0$).

For practical applications, therefore, it is sufficient to determine the loss and the mode structure only for the lowest loss modes, which means that we only have to calculate the envelope of the curves in Fig. 7.20. The calculated loss factor per round trip of the lowest loss mode for unstable resonators in circular and rectangular symmetry are presented in Fig. 7.21. In these graphs, the loss factor is plotted versus the equivalent Fresnel number N_{eq}, which is related to the effective Fresnel number via:

$$N_{eq} = N_{eff}\sqrt{G^2 - 1} \tag{7.23}$$

By using the equivalent Fresnel number as a mode parameter, the mode crossing points are characterized by integral values of N_{eq}. As the intensity distributions in Fig. 7.22 indicate, the mode structure suddenly changes if the Fresnel number is slightly increased around an integral value of N_{eq}. Since the two modes have complementary intensity profiles and nearly the same diffraction losses, they can oscillate simultaneously. In order to attain true single transverse mode operation in an unstable resonator, it, therefore, is recommended to choose half integral values of the equivalent Fresnel number because the loss difference between modes is a maximum in these areas (Fig. 7.23).

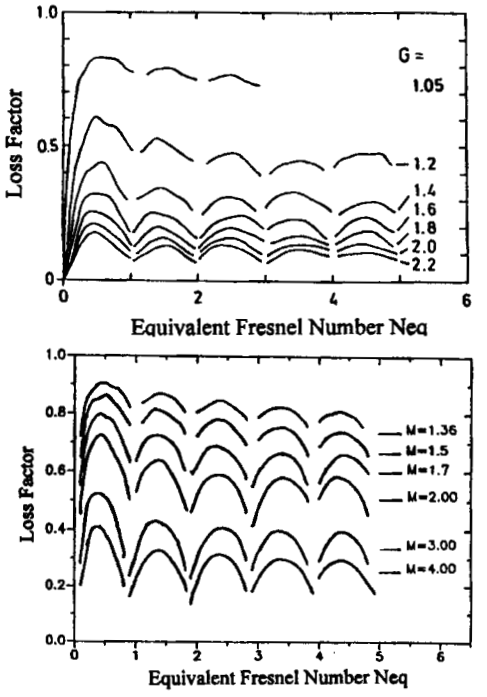

Fig. 7.21 Calculated loss factor per round trip of the lowest loss modes as a function of the equivalent Fresnel number N_{eq}. a) circular symmetry with mirror radius a, b) rectangular symmetry with mirror width $2a$, one-dimensional loss factor V_x, the total loss factor is $V=V_xV_y$ [3.129] (Chapman & Hall 1992).

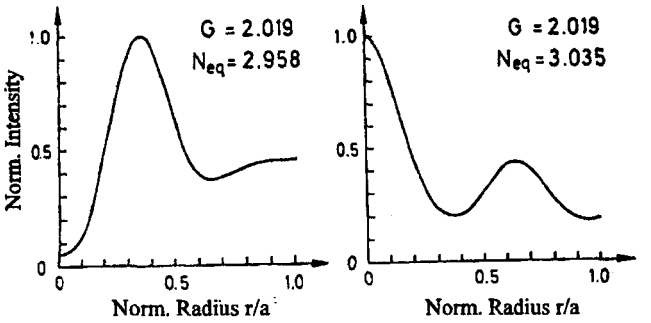

Fig. 7.22 Calculated radial intensity distributions on the confined mirror at an equivalent Fresnel number $N_{eq}=3$ for a magnification of $M=3.75$ [3.116] (© AIP 1988).

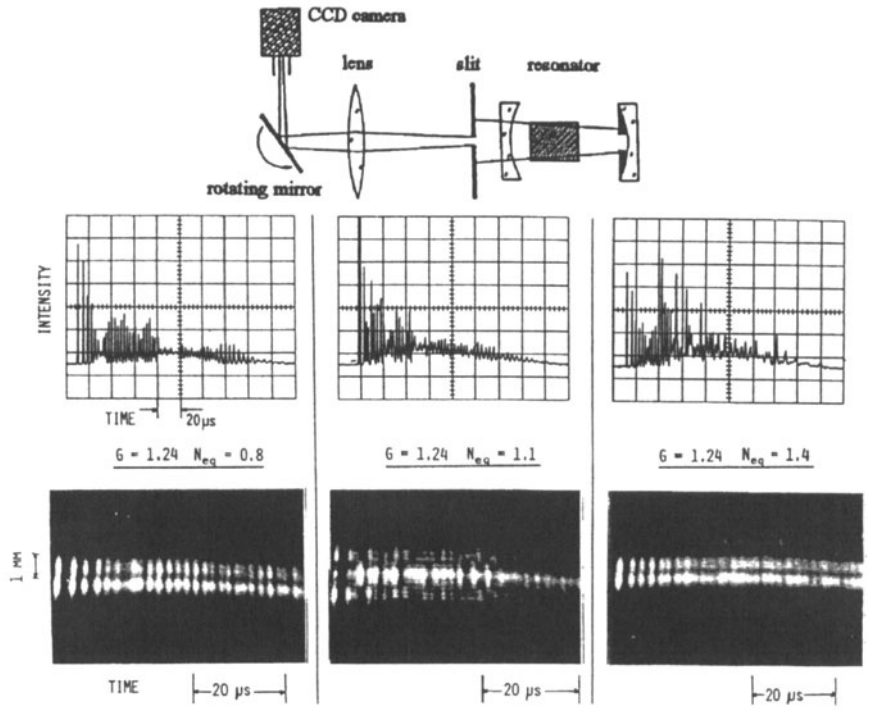

Fig. 7.23 Time resolved measurement of the radial mode structure of an Nd:YAG laser with an unstable resonator. The drawing depicts the experimental set-up. The upper row represents the temporal laser emission, the photographs below show the corresponding radial intensity distributions. The simultaneous oscillation of two transverse modes is observed at $N_{eq}=1.1$ (photograph in the middle) [3.116] (© AIP 1988).

Figure 7.24 shows measured radial intensity distributions at the plane of the output coupler in comparison to the theoretical profiles. The radius a of the output coupler and the geometrical beam radius Ma are indicated. With increasing Fresnel numbers the mode structures exhibit more side lobes and will approach a homogeneous profile for very large Fresnel numbers. Note that the geometrical beam radius Ma is quite a good approximation for the lateral extent of the modes. Similar to the mode structures, the loss factors converge to the geometrical loss factor for large Fresnel numbers (Fig. 7.25).

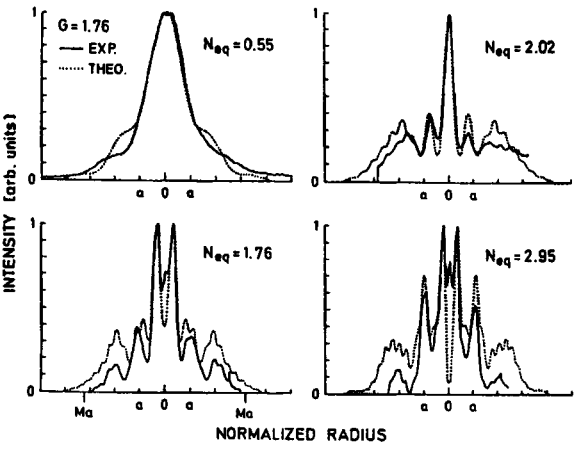

Fig. 7.24 Measured radial intensity distributions at the plane of the output coupler of unstable resonators in circular symmetry with $G=1.76$ ($M=3.21$) and different equivalent Fresnel numbers. The profile within the radius a is reflected by the mirror, the outer portion of the mode is coupled out. The dotted lines are the numerically calculated distributions (pulsed Nd:YAG laser) [3.116] (© AIP 1988).

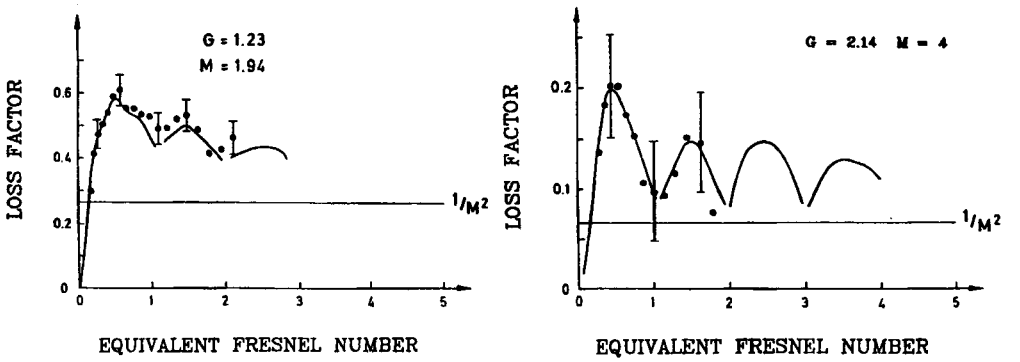

Fig. 7.25 Measured and calculated loss factors per round trip of unstable resonators in circular symmetry for different magnifications M as a function of the equivalent Fresnel number (pulsed Nd:YAG laser) [3.116] (© AIP 1988).

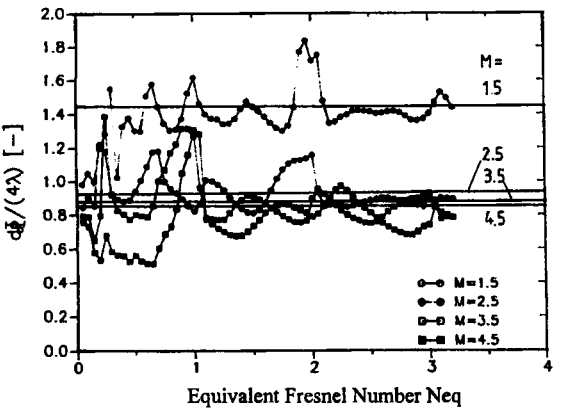

Fig. 7.26 Calculated normalized beam parameter products $d_0\Phi/(4\lambda)$ (86.5% power content) of unstable resonators in circular symmetry as a function of the equivalent Fresnel number for different magnifications M. The corresponding values for a homogeneous annular ring (Fig. 7.14) are indicated by the horizontal lines.

The mode structure at the output coupler not only influences the loss factor, but also affects the beam quality of the unstable resonator. Figure 7.26 shows beam parameter products (86.5% power content) as a function of N_{eq} and M, taking into account the mode structure in the near field. The comparison with the beam parameter products obtained by approximating the near field by a homogeneous ring profile indicates that the incorporation of the mode structure at the output coupler generally improves the beam quality (except close to integral values of N_{eq}). Furthermore, the power content in the central peak is increased as compared to the far field of an annular ring (Fig. 7.27, cf. Fig. 7.14).

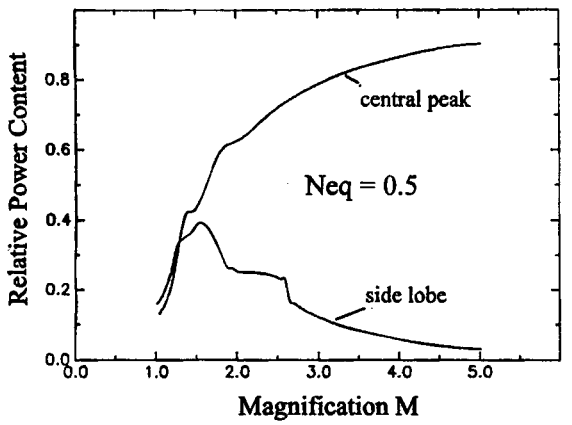

Fig. 7.27 Calculated power content in the central peak and in the side lobe of the far field intensity distribution as a function of the magnification (circular symmetry, $N_{eq}=0.5$).

7.3.2 Applications of Unstable Resonators

The main advantage of unstable resonators is the adaptation of the beam radius inside the resonator by changing the mirror radius a. Since single transverse mode operation is not linked to the size of the mirror, as is the case for stable resonators, beam qualities close to the diffraction limit can be attained even for gain media with very large cross sections. In contrast to stable resonators, a high mode volume and a high beam quality can be realized simultaneously. This sounds too good to be true. So what are the drawbacks ?

First of all, the power content in the side lobes of the far field might cause problems in specific applications. In order to minimize the power content in the side lobes the magnification has to be chosen as high as possible. This, however, requires an active medium with a high gain. It therefore makes no sense to use an unstable resonator in a HeNe laser, since the gain is too low to obtain a good laser efficiency. Secondly, the output power of unstable resonators generally is 20%-30% lower as compared to a stable resonator in multimode operation. This is due to a lower fill factor in combination with additional diffraction losses induced by the rim of the active medium. If one is more interested in the output power than in attaining an excellent beam quality, it is therefore more advantageous to use a stable resonator in multimode operation. This preference of multimode stable resonators is also due to their easier alignment and their lower sensitivity to mirror misalignment.

Unstable resonators have found application in high power CO_2 lasers 3.60,3.64,3.66,3.69,3.83,3.122] and excimer lasers [3.92,3.102,3.119], both of which generally exhibit a high gain and a large cross section of the active medium. Unstable resonators are also used in pulsed solid state lasers [3.85,3.106,3.111,3.125-3.129,3.137,3.146,3.152,3.156,3.163-3.169]. Unfortunately, the thermal lensing of the solid state laser materials deteriorates the beam quality and makes beam handling quite difficult, as will be discussed in Chapter 12. It is for this reason that most applications of unstable resonators in solid state laser engineering are limited to low power Q-switch systems. The utilization of unstable resonators in diode lasers [3.124], dye lasers [3.171], and free electron lasers [3.100,3.107,3.114] has also been reported.

7.4 Misalignment Sensitivity

All geometrical relations presented in Sec. 5.4 for stable resonators also apply to unstable resonators. Since mirror 2 is always unconfined, the additional losses occur at the output coupling mirror 1 due to a shift Δ_{1j} of the optical axis with respect to the center of mirror 1. If mirror 2 is tilted by an angle α_2 and the output coupling mirror exhibits a radius a, the relative shift is given by (Fig. 7.28, see also Fig 5.47):

$$\frac{\Delta_{12}}{a} = \frac{L\alpha_2}{a}\,\frac{2}{|G-1|} \tag{7.24}$$

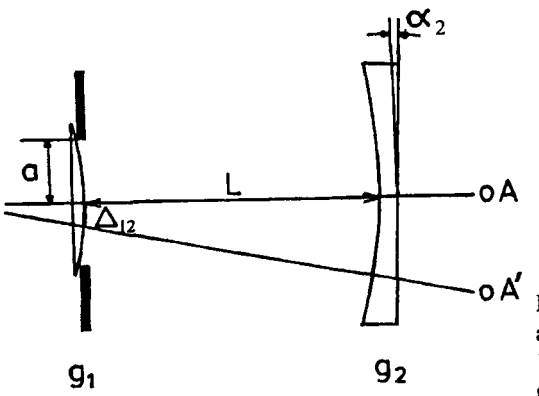

Fig. 7.28 Misalignment of mirror 2 induces a shift Δ of the optical axis (oA) on mirror 1. Additional diffraction losses are generated at the confined mirror 1.

If mirror 1 is tilted by an angle α_1, the corresponding relation reads:

$$\frac{\Delta_{11}}{a} = \frac{Lg_2\alpha_1}{a}\frac{2}{|G-1|} \tag{7.25}$$

We see that a tilt of the unconfined mirror by the angle α_2 is equivalent to the misalignment of the output coupling mirror by the angle $\alpha_1=\alpha_2/g_2$. These two geometrical relations already provide us with valuable information on the tilt sensitivity of unstable resonators:

- the misalignment sensitivity gets lower if the equivalent g-parameter G or the magnification M is increased.
- negative branch resonators ($G<-1$) are less sensitive to mirror tilt than positive branch resonators. For a magnification of $|M|=2$, we can expect a nine times lower sensitivity in the negative branch (assuming equal length L and equal mirror radius a).

Similar to stable resonators, unstable resonators experience a parabolic increase of the losses if one of the resonator mirrors is tilted [3.60,3.68,3.79,3.89,3.118,3.129]. However, the diffraction losses of unstable resonators can also increase at higher tilt angles as shown in Fig. 7.29. The resulting loss factor minima can be related to a switching of transverse modes similar to the mode switching of the aligned resonator at integer equivalent Fresnel numbers N_{eq}. Using the shift Δ of the optical axis, we can define two new equivalent Fresnel numbers $N_{eq}^{\pm}$ with:

$$N_{eq}^{\pm} = \frac{(a\pm\Delta)^2}{2Lg_2\lambda}\sqrt{G^2-1} \tag{7.26}$$

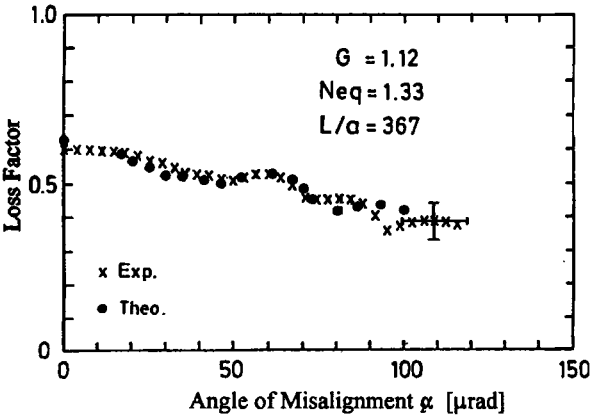

Fig. 7.29 Measured loss factor per round trip of a circularly symmetric unstable resonator for misalignment of the unconfined mirror 2 (Nd:YAG rod laser). The dots represent a numerical calculation using diffraction integrals [3.118] (© Taylor & Francis 1988).

The tilt angles at which the mode crossings occur can be related to integer values of this newly defined equivalent Fresnel number. For the misalignment of the unconfined mirror, the loss factor minima occur at the angles:

$$\alpha_{2,p} = \frac{(G-1)a}{2L}\left[\mp 1 \pm \sqrt{1 - \frac{|N_{eq}-p|}{|N_{eq}|}}\right] \tag{7.27}$$

with p being an integer. The upper sign holds for $p>|N_{eq}|$, the lower sign for $p<|N_{eq}|$. For the measurement shown in Fig. 7.29, Eq. (7.27) yields 21.7μrad (p=*1*), 37 μrad (*p=2*), and 82μrad (*p=3*), which is in good agreement with the experimental data.

In general, the tilt angle at which the first mode crossing occurs is greater than the tilt angle $\alpha_{10\%}$ at which the losses have increased by 10%. Similar to stable resonators, we can therefore define a parabolic dependence of the loss factor V on the angle of misalignment:

$$V(\alpha) = V(0)\left[1 - 0.1\left(\frac{\alpha}{\alpha_{10\%}}\right)^2\right] \tag{7.28}$$

As was already done in Sec. 5.4 for the misalignment of stable resonators, it is convenient to introduce the misalignment parameter $D=L\alpha_{10\%}/a$ to quantify the misalignment sensitivity of unstable resonators. The misalignment parameter depends only on the equivalent g-parameter G and the absolute value of the equivalent Fresnel number N_{eq}. Figure 7.30 presents calculated misalignment parameters for the misalignment of the unconfined mirror 2 as a function of the equivalent Fresnel number for both positive branch and negative branch unstable resonators. The calculations were performed by numerically solving integral

equation (5.85). These graphs enable us to determine the 10% angles of any unstable resonator. Note that the 10% tilt angle of the confined mirror 1 can also be determined by applying the above mentioned equivalency relation between the tilts of the two mirrors. As we already found in our preliminary geometrical result (7.24), the misalignment sensitivity becomes lower for high magnifications and small ratios of resonator length L to mirror radius a. Furthermore, a low Fresnel number is advantageous for the stability of an unstable resonator. Figure 7.30 also confirms the lower sensitivity of negative branch resonators predicted by our geometrical analysis!

How does this compare to the misalignment sensitivity of stable resonators ? The misalignment parameters for stable resonators in fundamental mode operation with adapted aperture radius ($a=1.3w$, w: Gaussian beam radius at the aperture) and for positive branch unstable resonators with $N_{eq}=0.5$ are presented in Fig. 7.31. This graph indicates that the misalignment parameters are comparable. However, in order to get a high mode volume of the Gaussian beam in the stable resonator, an equivalent g-parameter G between 0.95 and 1.0 or a large resonator length is required. Considering this, the 10%-angle of stable resonators in fundamental mode operation, therefore, is several times smaller as compared to unstable resonators.

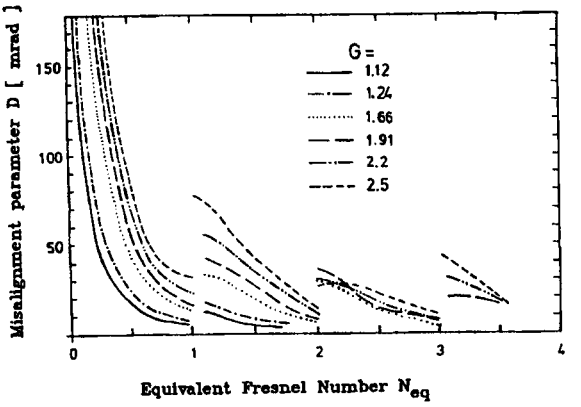

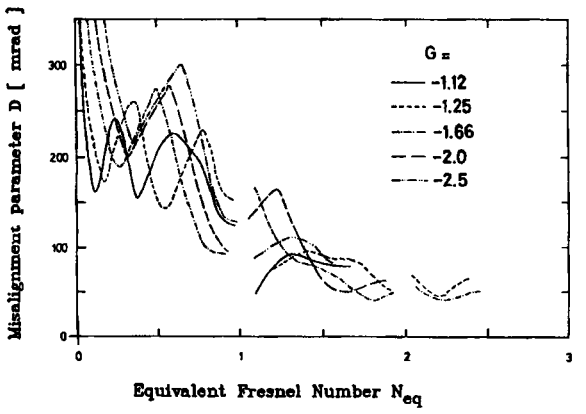

Fig. 7.30 Calculated misalignment para-meter $L\alpha_{10\%}/a$ as a function of the equivalent Fresnel number for misalignment of the unconfined mirror of unstable resonators in circular symmetry. a) positive branch, b) negative branch [3.118] (© Taylor & Francis 1988).

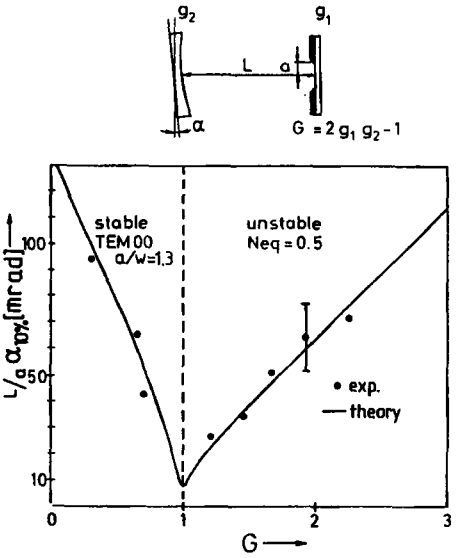

Fig. 7.31 Measured and calculated misalignment parameter of stable resonators in fundamental mode operation with adapted aperture radius a and positive branch unstable resonators with equivalent Fresnel number N_{eq} as a function of the equivalent g-parameter G. The unconfined mirror 2 is tilted (circular symmetry).

Example:

Confocal resonator with M=2 (g_1=1.5, g_2=0.75, G=1.25, L=0.5m, λ=1.064μm)
In order to fill an active medium of diameter 6.35mm we need a mirror radius a of 1.58mm. This results in an equivalent Fresnel number of $N_{eq}=2.36$. For this resonator the misalignment parameter in Fig. 7.30 is 20 mrad. This results in a 10%-angle of 63 μrad for the unconfined mirror. If the output coupling mirror is misaligned the 10%-increase of the loss occurs at a tilt angle of 84μrad (=63μrad/g_2).

Now let us design a stable resonator in fundamental mode operation having a comparable mode volume and the same resonator length. The Gaussian beam radius w_i at mirror i is given by (see Sec. 2.8.2):

$$w_i^2 = \frac{2Lg_j\lambda}{\pi\sqrt{1-G^2}}, \quad i,j=1,2 \; ; \; i \neq j$$

We place the active medium close to mirror 1. In order to completely fill the medium, the Gaussian beam radius w_1 has to be 1.3 times smaller than the radius of the medium, resulting in w_1=2.44mm (the radius of the medium is the aperture radius a). We choose a mirror radius of mirror 2 of -0.25m. With this choice all other resonator parameters are defined: $g_2=3.0$, $G=0.985$, $g_1=0.331$. According to Fig. 7.31 (or Fig. 5.49), the misalignment parameter for mirror 2 is about 8mrad. This results in 10%-angles of 51μrad for mirror 2 and 17μrad for mirror 1. This resonator would be several times more sensitive to misalignment than the unstable resonator!

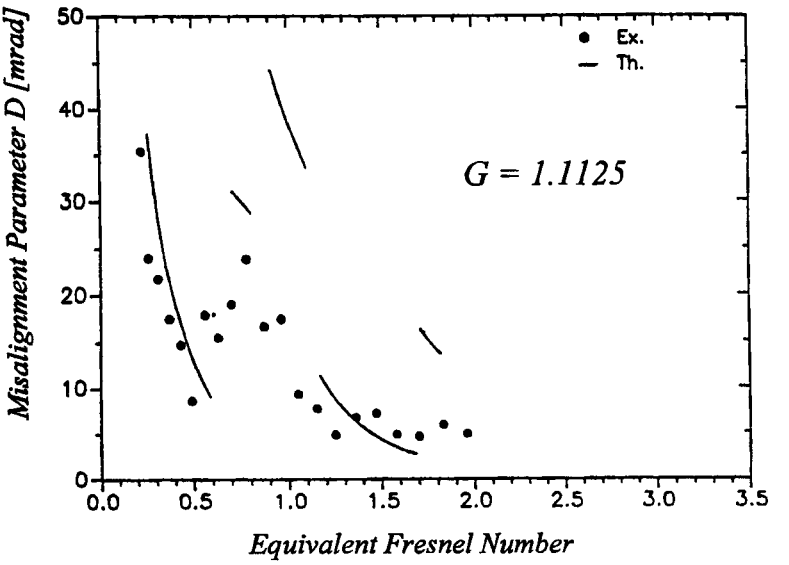

Fig. 7.32 Measured and calculated misalignment parameter as a function of the equivalent Fresnel number for unstable resonators in rectangular symmetry with magnification $M=1.6$ (Nd:YAG slab laser) [S.7].

In rectangular symmetry, the misalignment sensitivity of unstable resonators is comparable to the circularly symmetric ones as a comparison of Fig. 7.32 and Fig. 7.30a indicates.

The reader should keep in mind that the misalignment of unstable resonators increases the output coupling. This is in contrast to stable resonators in which the output coupling remains constant and the increase in loss is due to clipping of the beam at an aperture. It is for this reason that the influence of mirror misalignment on the output power is quite different for the two resonator types. In contrast to stable resonators in which a mirror tilt is equivalent to a decrease of output power, unstable resonators may exhibit an increase of power. This increase can be observed if the aligned resonator is undercoupled, which means that the output coupling is too low for the given small-signal gain of the active medium. This interesting property will be discussed in more detail in Chapter 14. We will see that the increase in output coupling results in a misalignment sensitivity of the output power that is twice as low as compared to the sensitivity of the power of stable resonators in fundamental mode operation, assuming the same 10%-angle for the loss for both resonators. A similar statement holds for the shape of the far field intensity distribution. Even for tilt angles much higher than the 10%-angle, the shape stays almost constant, as the measured intensity distributions in Fig. 7.33 indicate. For stable resonators in fundamental mode operation, the far field structure already exhibits a noticeable asymmetry at the 10%-angle.

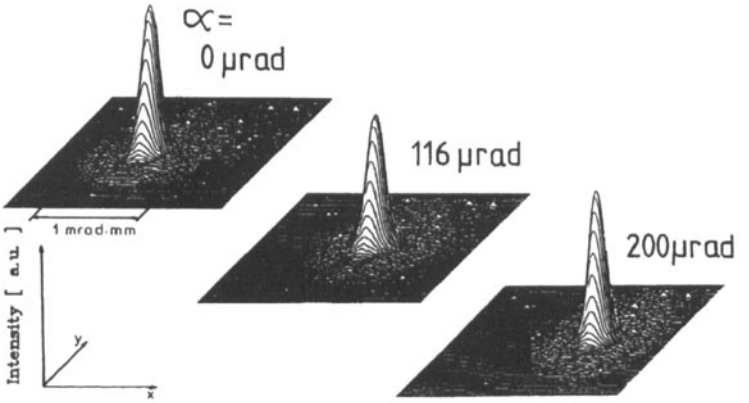

Fig. 7.33 Measured, normalized intensity distributions in the far field of a positive branch unstable resonator for different tilt angles of the unconfined mirror ($G=1.75$, $N_{eq}=2.85$, $L=0.32m$, $a=1mm$, $\lambda=1.064\mu m$, Nd:YAG rod laser). The 10%-angle $\alpha_{10\%}$ is 50μrad [3.118] (© Taylor & Francis 1988).

7.5 Unstable Resonators in Off-Axis Geometry

Unstable resonators in rectangular geometry exhibit high side lobes in the far field, even for high magnifications ($M>2$). This is due to the fact that the far field is determined by diffraction at a double slit which leads to a strong modulation of the intensity distribution in the far field (see Fig. 7.15b). Fortunately, the side lobes can be decreased considerably if the radiation is coupled out at one side of the high reflecting output coupling mirror [3.1,3.129]. This can be accomplished by misaligning both resonator mirrors in such a way that the optical axis is positioned along a corner of the active medium rather than choosing the symmetry axis of the medium as the optical axis (Fig. 7.34). If spherical mirrors are used the beam is magnified along the x- and the y-axis during a round trip but only in one direction. Accordingly, the beam is coupled out at one side of the output coupler only. The one-dimensional intensity distribution in the far field is now given by the Fourier transform of an illuminated single slit (see Sec. 2.2.1). The effect of this special output coupling scheme on the mode structure and the far field intensity distribution is presented in Fig. 7.35 for a confocal unstable resonator with magnification $M=1.5$. The power content in the side lobes of the far field is clearly reduced resulting in an improvement of the beam quality by a factor of 2. Note that in off-axis geometry the near field experiences diffraction losses at the edge of the active medium (hatched area in the upper right graph). These additional losses can be minimized by adjusting the mirror alignment so that the optical axis is slightly moved outside the active medium. Since the off-axis unstable resonator can be viewed as a misaligned on-axis resonator, the diffraction losses are higher as compared to on-axis unstable resonators in rectangular symmetry (Fig. 7.36, see Fig. 7.21b for a comparison).

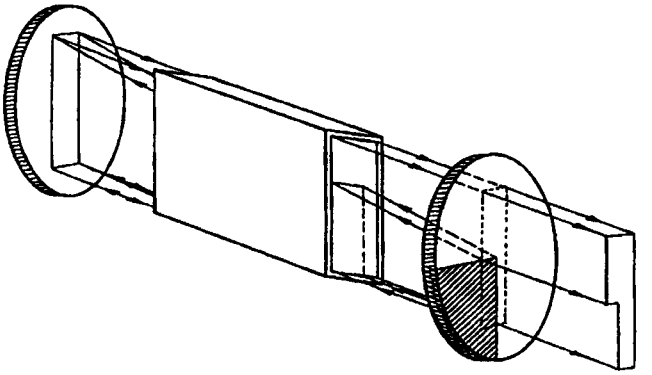

Fig. 7.34 Confocal unstable resonator with spherical mirrors in off-axis geometry. The optical axis is positioned along the lower left corner of the active medium. The hatched area marks the HR coating of the output coupling mirror [3.129] (© Chapman and Hall 1992).

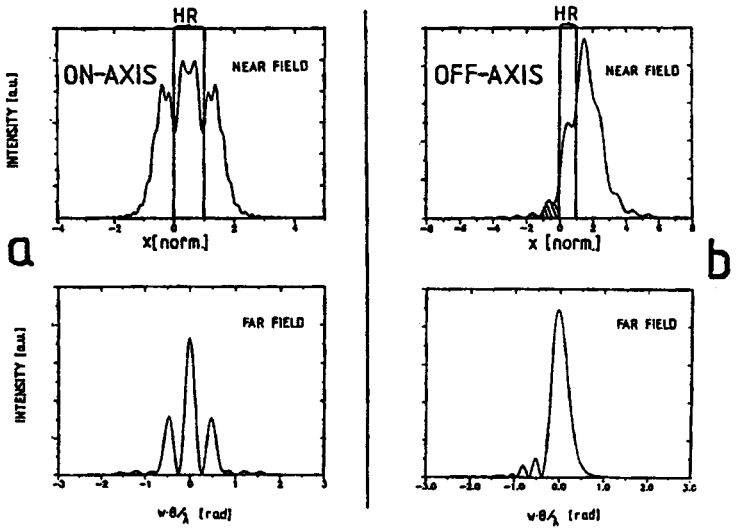

Fig. 7.35 Calculated intensity distributions in the near field and in the far field of an unstable resonator with magnification $M=2$, both in on-axis and in off-axis geometry. The near field inside the resonator at the plane of the output coupler, is shown (HR indicates the high reflecting area) [3.129] (© Chapman and Hall 1992).

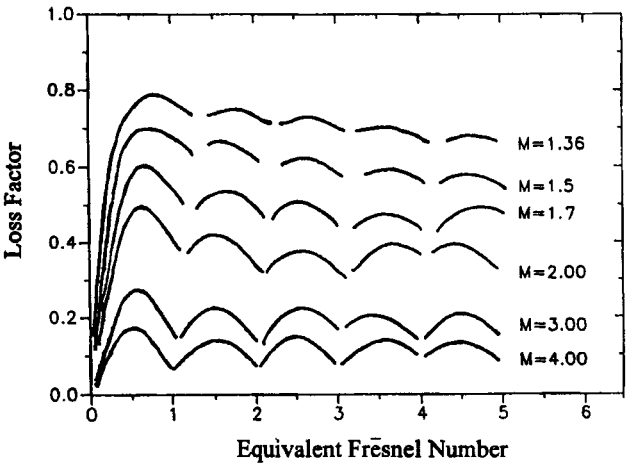

Fig. 7.36 Calculated one-dimensional loss factors of unstable resonators in off-axis geometry as a function of the equivalent Fresnel number $N_{eq} = a^2\sqrt{G^2-1}/(2Lg_2\lambda)$ (a: width of the HR coating on the output coupler hit by the beam). The curve parameter is the magnification M (see also Fig. 7.21b).

In spite of the asymmetry of the L-shaped intensity distribution coupled out of the resonator, the intensity distribution in the far field is symmetric with respect to the x-axis and the y-axis. The slight asymmetry in the far field intensity distribution in Fig. 7.35 is a result of the near field mode structure; if the near field were a perfect L with homogeneous illumination, the focus would be completely symmetric. Figure 7.37 presents photographs of the near field and the far field of a Nd:YAG slab laser with an unstable resonator with magnification $M=1.4$ in off-axis geometry. The comparison of the beam quality of on-axis and off-axis unstable resonators shown in Fig. 7.38 clearly indicates the advantages of the off-axis geometry.

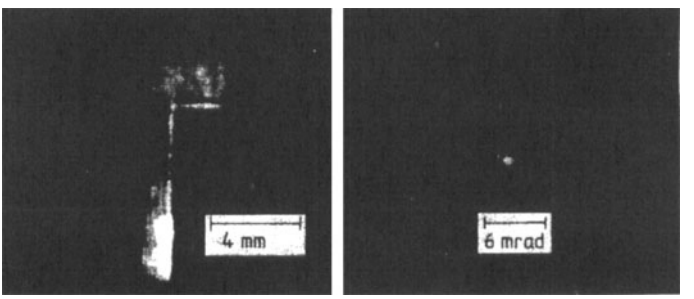

Fig. 7.37 Photographs of the near field and the far field intensity distributions of a confocal unstable resonator in off-axis geometry with $M=1.4$ (Nd:YAG slab laser, $\lambda=1.064\mu m$, cross sectional area of the slab: 4x12 mm^2) [3.129] (© Chapman and Hall 1992).

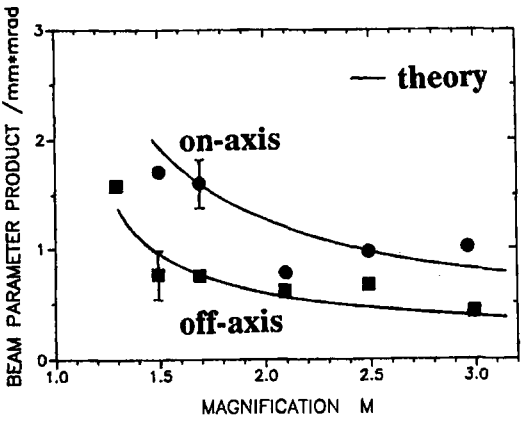

Fig. 7.38 Measured and calculated beam parameter products $d\Phi/4$ (d: waist width, Φ: full angle of divergence, both defined by the 86.5% power content) of unstable resonators in on-axis and in off-axis geometry versus the magnification M (Nd:YAG laser, $\lambda = 1.064\mu m$) [3.129] (© Chapman and Hall 1992).

For active media with rectangular cross section the off-axis geometry is the preferred means to attain good beam quality. Since the aspect ratio of the medium (ratio of height to width) is generally high (for solid state slab lasers and CO_2 slab lasers the aspect ratio is 4-6 and 5-10, respectively) it is common to apply the off-axis unstable resonator scheme only in the direction of the larger dimension. In the perpendicular direction (width) a stable resonator (solid state) or a waveguide resonator (CO_2) is usually chosen [5.80,5.104]. Since the width is on the order of millimeters it is possible to obtain beam qualities near the diffraction limit by using the latter two resonator concepts. A detailed discussion on these so called hybrid resonators is given in Chapter 19. Figures 7.39 and 7.40 show layout and performance of a diode-pumped Nd:YAG slab laser using an off-axis unstable resonator along the slab width and a stable resonator along the thickness of the slab.. By using a variable reflectivity mirror (VRM) as the output coupler, a beam propagation factor M^2 of less than 1.2 was attained in the unstable direction [3.179]. Similar results have been reported at even higher power levels [3.173-175] and also for Vanadate slabs [3.177,3.178].

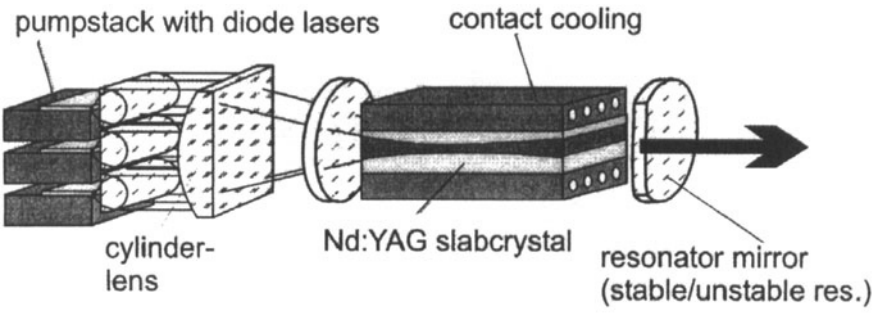

Fig. 7.39 End-pumped Nd:YAG slab laser with off-axis unstable resonator [3.180].

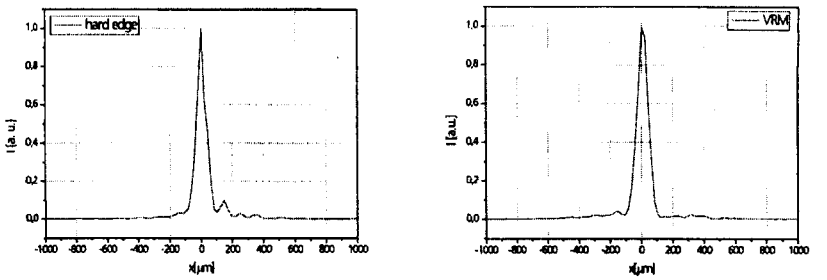

Fig. 7.40 Measured focus intensity distribution for the slab laser of Fig. 7.39 in the unstable resonator direction, with a hard edge (left) and a variable reflectivity output coupler (VRM, right). Output power in both cases was 60W, magnification :1.7 for hard edge and 1.2 for VRM [3.180].

It is also possible to apply the off-axis concept to circularly symmetric media (Fig. 7.41). Unfortunately, it is very difficult to manufacture glass substrates exhibiting the aspheric shapes required for this resonator concept. It is for this reason that circularly symmetric off-axis resonators have only been realized in CO_2 lasers for which copper mirrors of any shape can be made using diamond milling [3.130]. The basic principle of the resonator set-up can be understood if we imagine a one-dimensional off-axis unstable resonator in rectangular symmetry whose cylindrical mirrors are bent to form a tube. The output coupling mirror now exhibits an annular shape and the laser beam emerges from the resonator through the central aperture. Thus, the far field is similar to the Fraunhofer diffraction pattern of a circular aperture having much lower side lobes as compared to an on-axis unstable resonator (Fig. 7.42). Note that for a given magnification M, the output coupling losses are lower in the off-axis geometry. Instead of $1/M^2$ for the on-axis resonator, the geometric loss factor is now given by (Fig. 7.43):

$$V = \frac{2}{M} - \frac{1}{M^2} \tag{7.29}$$

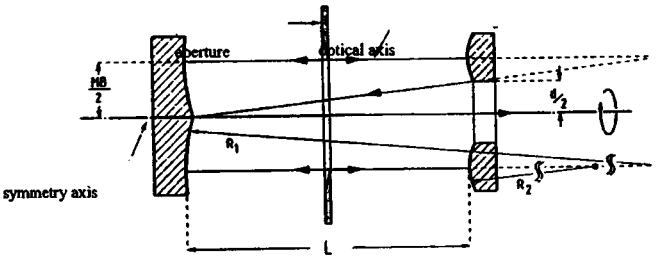

Fig. 7.41 The off-axis unstable resonator in circular geometry [S. 8].

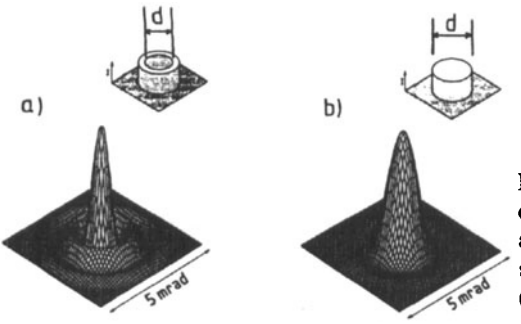

Fig. 7.42 Calculated far field intensity distributions for confocal on-axis (a) and off-axis (b) unstable resonators in circular symmetry. The magnification is $M=1.5$ ($d=20mm$, $\lambda=10.6\mu m$) [S.8].

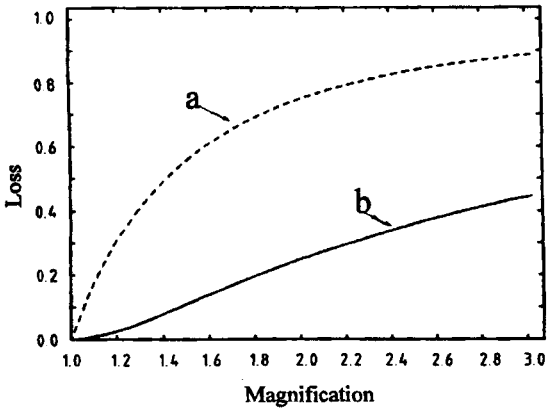

Fig. 7.43 Geometric loss per round trip for circularly symmetric unstable resonators in on-axis (a) and off-axis geometry (b) as a function of the magnification [S.8].

7.6 Unstable Resonators with Homogeneous Output Coupling

The side lobes in the far field of unstable resonators are caused by diffraction off the edge of the output coupling mirror in combination with the annular shape of the near field. A method to overcome this disadvantage is to transmit the laser beam through a partially reflecting unconfined mirror (Fig. 7.44). The beam size is defined by an aperture in front of the high reflecting mirror which replaces the output coupler described in previous sections. Similar to the off-axis resonators, the far field distribution is given by the Fraunhofer diffraction pattern of a round aperture which exhibits smaller side lobes. However, due to the mode structure at the aperture, which for low equivalent Fresnel numbers exhibits a Gaussian-like field distribution, the power content in the side lobes is even smaller.

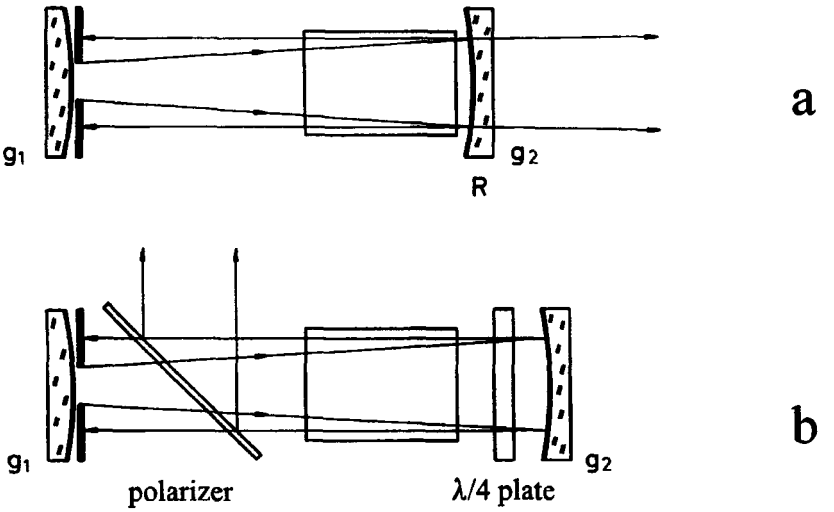

Fig. 7.44 Unstable resonators with homogeneous output coupling. a) using a partially reflecting mirror 2, b) using a polarizer with a rotatable quarter wave plate to vary the output coupling.

The laser beam can be described as a Gaussian beam to a good approximation. Unfortunately, the price to be paid for this improvement is a considerable decrease of output power because the diffraction loss of the unstable resonator represents a true loss. It is recommended to use a low magnification to keep this loss as low as possible. This resonator concept, therefore, is only suitable for applications in which a perfect beam quality and a Gaussian intensity distribution is more important than the optimization of the laser efficiency (e.g. as a master oscillator to feed the beam into an amplifier chain) [5.29]. Unstable resonators with homogeneous output coupling are used for active media with high gain and small emission wavelengths (Q-switched solid state lasers and excimer lasers). For these lasers no other resonator concept exists that combines near diffraction limited focusability with a high efficiency. A common stable resonator in fundamental mode operation might not provide the output power required. Note that replacing the aperture by a high reflecting flat mirror in order to decrease the losses will not work since the two mirrors will then form a stable resonator depleting the gain in the outer area of the medium.

7.7 Unstable Resonators with Variable Reflectivity Mirrors

7.7.1 Resonator Properties

A better way than using homogeneous output coupling techniques to decrease the power content in the side lobes of the far field of unstable resonators is the utilization of output coupling mirrors with a variable reflectivity profile [3.131-3.171]. The reflectivity profile which generally exhibits a maximum at the center improves the beam quality by two effects. The diffraction of the power into the side lobes is considerably decreased by replacing the hard edge by a continuous transition from high to low reflectance. Furthermore, the center reflectivity and the shape of the profile can be varied to generate a specified intensity profile in the near field (e.g. flat top beams). Figure 7.45 shows the effect of the reflectivity profile on the near field and the far field intensity distributions of a confocal unstable resonator in circular symmetry with magnification $M=2$. The parabolic and the Gaussian profile both decrease the power content in the first side lobe from 25% to about 3-4%. The specific shape of the reflectivity profile is only of secondary importance, especially if the center reflectivity is chosen lower than 100%. However, in order to maximize the fill factor, steeper profiles are preferred since the mode with its correspondingly steeper slopes can be better adapted to the active medium. From 1985 to 1995 much effort was spent to develop coating techniques for generating variable reflectivity mirrors (VRM) exhibiting Gaussian, super-Gaussian, and parabolic reflectivity profiles [3.140,3.151,3.154,3.160,3.162, 3.166, 3.168].

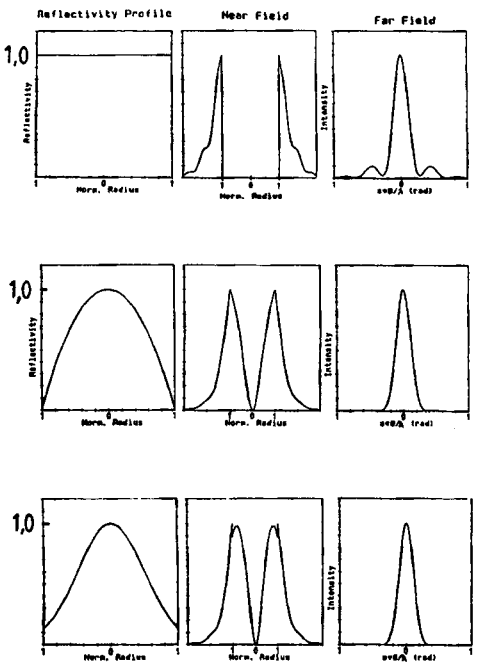

Fig. 7.45 Calculated intensity distributions in the near field and the far field of a confocal unstable resonator with $M=2$ and $N_{eq}=0.5$ for different reflectivity profiles of the output coupler.

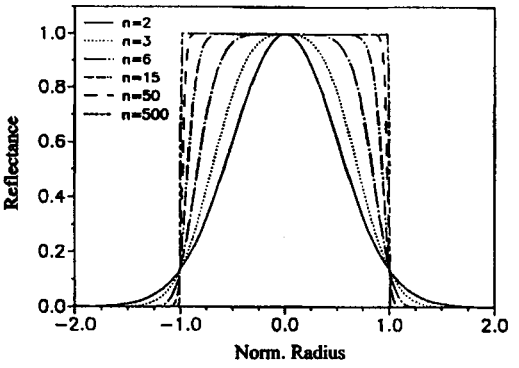

Fig. 7.46 Super-Gaussian reflectivity profiles for different indices n as a function of the radius [S.9].

Super-Gaussian Mirrors

The VRMs most commonly used exhibit a super-Gaussian reflectivity profile which in circular symmetry reads:

$$R(r) = R_0 \exp\left[-2\left(\frac{r}{w}\right)^n\right] \tag{7.30}$$

with:
- R_0: center reflectivity
- w: profile radius
- n: super-Gaussian index
- r: radial coordinate

The super-Gaussian index n determines the shape of the reflectivity profile. For $n=2$ the profile is Gaussian and with increasing n the slopes become steeper until the hard edge profile is approached in the limit $n\text{-->}\infty$ (Fig. 7.46).

The mode properties can be evaluated by using the stationary condition for the electric field. If $E_1(r)$ denotes the electric field hitting the output coupling mirror, the electric field after one round trip reads (we treat the round trip by magnifying the field by the magnification M):

$$E_2(r) = \frac{1}{M} E_1(r/M) \sqrt{R(r/M)} \tag{7.31}$$

The stationary condition $E_2(r)=\gamma E_1(r)$ with γ being the eigenvalue yields:

$$\gamma E_1(r) = \frac{1}{M} E_1(r/M) \sqrt{R(r/M)} \tag{7.32}$$

After insertion of the super-Gaussian reflectivity profile (7.30), the stationary electric field can be calculated. The corresponding intensity profile is given by:

$$I(r) = I_0 \exp\left[-2\left(\frac{r}{w_M}\right)^n\right] \tag{7.33}$$

with: $$w_M = w\,(M^n-1)^{1/n} \qquad M > 1 \tag{7.34}$$

The total loss factor per round trip reads:

$$V = \gamma\gamma^* = \frac{R_0}{M^2} \tag{7.35}$$

Thus, the intensity distribution at the output coupler inside the resonator is also super-Gaussian with a beam radius w_M. The intensity profile of the near field can be obtained by multiplying (7.33) with the intensity transmission *1-R(r)* of the VRM. Note that the loss factor per round trip is the same for all super-Gaussian indices and equal to the geometrical loss factor! This result can be verified if diffraction integrals are used to propagate the field inside the resonator. Figure 7.47 presents numerically calculated loss factors per round trip of unstable resonators with $M=2$ as a function of the equivalent Fresnel number for different super-Gaussian indices. Only for low equivalent Fresnel numbers can the beam propagation not be described by geometrical optics. This is to be expected since the purpose of the VRMs is the reduction of diffraction effects.

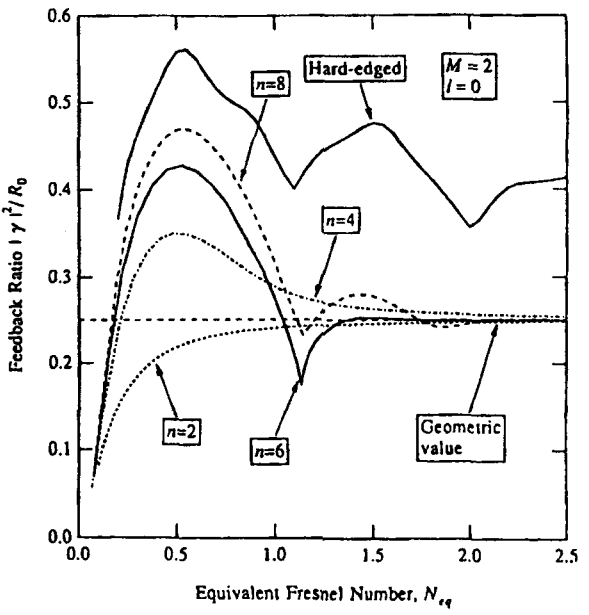

Fig. 7.47 Calculated loss factor per round trip of the lowest loss mode (ℓ=0) as a function of the equivalent Fresnel number for circularly symmetric unstable resonators with magnification $M=2$ using different super-Gaussian indices n [3.158] (© OSA 1992).

Ray Transfer Matrix for Gaussian Mirrors

For a mirror with a Gaussian reflectivity profile it is possible to define a ray transfer matrix which can be used to determine the beam properties by applying the ABCD law. Let us assume that a Gaussian beam with beam radius w_0 and infinite radius of curvature is incident on a Gaussian mirror with profile radius w and radius of curvature ρ. The beam parameters q_1,q_2 before and after the reflection read:

$$q_1 = -\frac{i\lambda}{\pi w_0^2} \quad , \quad q_2 = -\frac{2}{\rho} - \frac{i\lambda}{\pi}\left[\frac{1}{w_0^2} + \frac{1}{w^2}\right] \tag{7.36}$$
(7.37)

We know that the beam parameters transform according to the ABCD law:

$$q_2 = \frac{Aq_1 + B}{Cq_1 + D} \tag{7.38}$$

with A,B,C,D being the elements of the ray transfer matrix of the mirror. Since $B=0$ (no propagation) and $AD=1$, we find the ray transfer matrix of the Gaussian VRM to be:

$$M_{VRM} = \begin{pmatrix} 1 & 0 \\ -\frac{2}{\rho} - \frac{i\lambda}{\pi w^2} & 0 \end{pmatrix} = \begin{pmatrix} 1 & 0 \\ -\frac{2}{\rho} & 1 \end{pmatrix}\begin{pmatrix} 1 & 0 \\ -\frac{i\lambda}{\pi w^2} & 1 \end{pmatrix} \tag{7.39}$$

By using this matrix we can calculate the radius of curvature and the beam radius of the self-consistent Gaussian beam. Starting in front of the VRM (mirror 1), the ray transfer matrix for a round trip is given by:

$$M_{RT} = \begin{pmatrix} 4g_1g_2 - 1 - 2g_2 & 2Lg_2 \\ \frac{2}{L}[2g_1g_2 - g_1 - g_2] & 2g_2 - 1 \end{pmatrix}\begin{pmatrix} 1 & 0 \\ -\frac{i\lambda}{\pi w^2} & 1 \end{pmatrix} \tag{7.40}$$

Application of the ABCD law yields the stationary q-parameter (see Sec. 2.7.2). By using the assumption that the effective Fresnel number $N_{eff}=w^2/(2Lg_2\lambda)$ and the equivalent G-parameter $G=2g_1g_2-1$ are related by:

$$G > \frac{1}{2\pi N_{eff}} \tag{7.41}$$

the radius of curvature R and the beam radius w_M of the Gaussian beam in front of the VRM

result. Note that this assumption usually holds since in most lasers the effective Fresnel numbers are greater than one (see also Fig. 7.47 for the validity of (7.41)). A straightforward calculation yields the final results:

$$R = \frac{2Lg_2}{\sqrt{G^2-1} - G + 2g_2 - 1} \tag{7.42}$$

$$w_M = w\sqrt{M^2 - 1} \tag{7.43}$$

The radius of curvature R of the Gaussian beam represents the expected value for unstable resonators given by (7.9). The beam parameters of the Gaussian beam at any plane inside and outside the resonator can now be determined using the ABCD law for Gaussian beams. Although a Gaussian beam is an eigensolution, this resonator is not a stable resonator!

7.7.2 Production of VRMs

Variable reflectivity mirrors are produced by coating an AR-coated substrate with one or several layers having a decreasing thickness along the radius. The optical thickness in the center of each layer is preferably a quarter wavelength. The graded profile is generated by using a mask with diameter d located at a certain distance h on top of the substrate. The two mask parameters control the shape of the reflectivity profile. The deposition rate of the coating particles continuously decreases with increasing distance from the substrate's center (Fig. 7.48). With only one graded layer it is difficult to attain high center reflectances due to the limited availability of coating materials exhibiting a high enough refractive index (see Sec. 4.3.2).

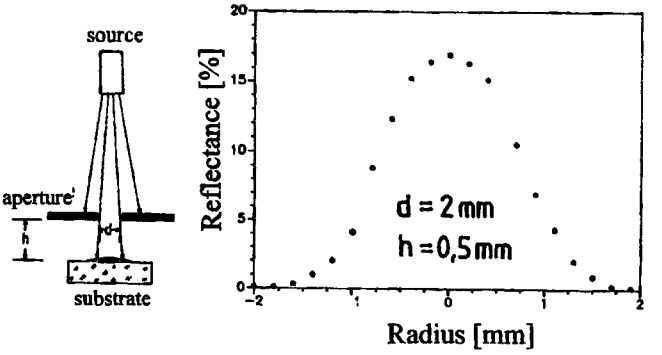

Fig. 7.48 Production of VRMs by coating through an aperture. The number of layers and the coating materials determine the center reflectivity. The aperture diameter d and the aperture distance h control the profile. The right figure shows the measured reflectivity profile of a single TiO_2 $\lambda/4$ layer on an AR-coated BK7 substrate.

For TiO_2(n=2.25), commonly used as high index material for lasers in the 1μm wavelength range, the maximum reflectance is about 50%. Laser mirrors with higher reflectance consist of multiple λ/4 layers, alternating high index and low index coating materials. If *N* denotes the number of high index layers and the thicknesses of all layers go to zero as we move away from the substrate center, the reflectivity profile exhibits *N-1* radial side lobes (Fig. 7.49). The phase shift associated with these maxima deteriorates the beam quality considerably. It is possible to get rid of the maxima by holding the layer thicknesses constant for radii greater than the radius of the first reflectance minimum. This can be accomplished by using a specially shaped rotating mask. Unfortunately, the rotation restricts this technique to mirrors with circular geometry.

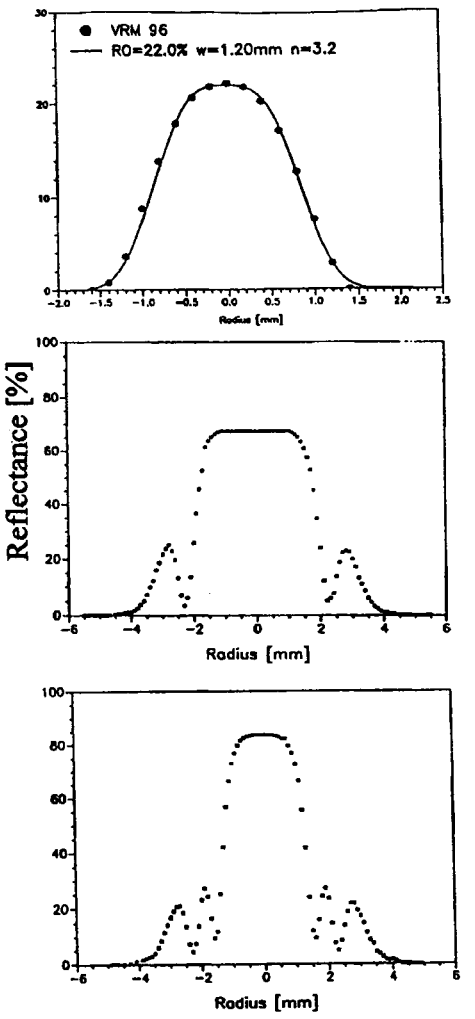

Fig. 7. 49 Measured reflectivity profiles of VRMs with one, three, and five λ/4 layers using SiO_2 as the low index material (L) and TiO_2 as the high index material (H) on a substrate S. Coating designs: a) air vH AR S, b) air vH vL vH AR S, c) air vH vL vH vL vH AR S [S.9].

A better method to generate VRMs with high center reflectances is to use a radially variable Fabry Perot interferometer made of dielectric layers (Fig. 7.50). A radially varying layer (etalon layer) is situated between two identical stacks of quarter wave layers, which determine the maximal possible reflectance. In the center, the maximum reflectivity is achieved due to the quarter wavelength spacing between the stacks, and at the positions where the etalon layer thickness goes to zero, the residual reflectance is that of the AR coating. By using this technique it is possible to generate VRMs with center reflectances as high as 95% [3.168]. Figure 7.51 shows a measured reflectivity profile of an FPI mirror for a Nd:YAG rod laser. VRMs in circular and rectangular geometry can be produces using this technique (Fig. 7.52).

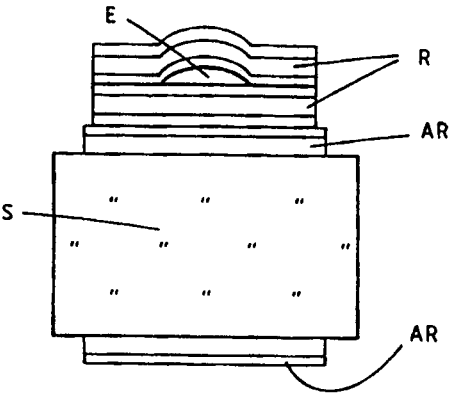

Fig. 7.50 Coating design of a variable Fabry Perot interferometer mirror (FPI mirror). S: substrate, AR: AR-coating, R: reflectance enhancing stack, E: etalon layer [S.9].

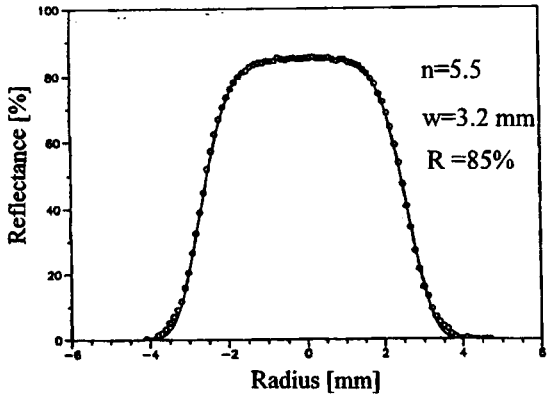

Fig. 7.51 Measured reflectance profile of an FPI mirror for a Nd:YAG laser at λ=*1.064μm*. The solid line represents a super-Gaussian profile with n=*5.5*, w=*3.2mm*, and R_0=*85%*. Coating design: quarter wavelength layers (air H L vH L H AR S), L:SiO_2, H:TiO_2 [S.9].

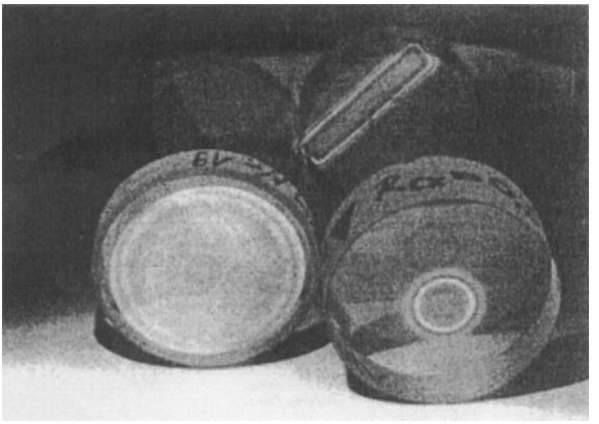

Fig. 7.52 Three VRMs for Nd:YAG lasers. The two 1" substrates in the front are used in rod lasers. The left mirror is an FPI mirror, the reflectance profile of the right mirror is shown in the middle graph of Fig. 7.49. The 2" substrate with the rectangular reflectivity profile is used in a slab laser [S.9].

7.7.3 Laser Properties of VRM Unstable Resonators

Owing to their excellent beam qualities, unstable resonators with variable reflectivity mirrors have found application in both gas and solid state lasers. VRMs are commercially available for a variety of laser wavelengths ranging from the visible to the infrared at 10.6μm. In solid state lasers, these resonators are mostly applied to low to medium power Q-switch systems [3.146,3.147,3.177,3.178], but successful operation in free running lasers with output powers in the kW range has also been reported [3.156,3.157,3.163-3.165,3.167,3.172-176]. Figure 7.53 presents results obtained for a high power Nd:YAG slab laser system using one oscillator and two amplifier stages. By using an unstable resonator with VRM this system provides a maximum output power of 2 kW at a repetition rate of 22 Hz. The VRM of the negative branch confocal unstable resonator exhibits a rectangular shape with profile radii w of 2mm and 7mm in the x- and y-direction, respectively. The beam quality is about ten times diffraction limited. The deterioration of the beam quality is caused by stress induced aberration in the active medium. With a flat-flat resonator an output power of 3 kW is obtained, but the beam quality along the y-direction is decreased by a factor of 25 (Fig. 7.53b). Near diffraction limited beam was generated with a diode side-pumped thin Nd:YAG slab laser with positive branch confocal unstable resonator in the wide direction (Fig.7.45). In the perpendicular direction, the spherical HR mirror generated a stable resonator with a Gaussian beam diameter inside the slab of about 0.4mm. The output coupler was a VRM with a Gaussian profile with 67% center reflectivity and a profile radius of w=3.5mm. A cw output power of 220W was reported at beam propagation factors of less than 1.5 in both directions (Fig. 7.55) [3.176].

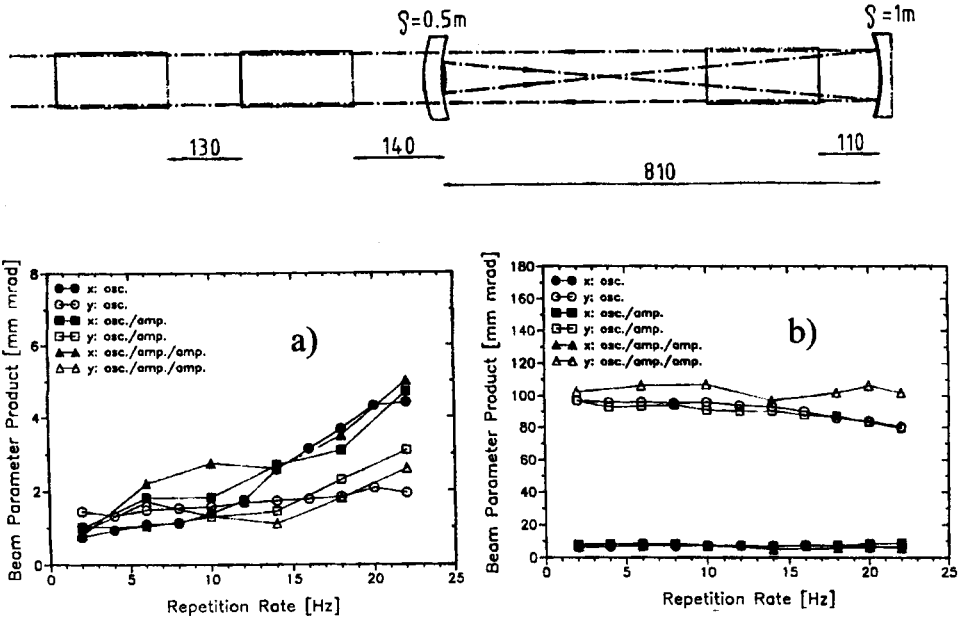

Fig. 7.53 Measured beam parameter products $d\Phi/4$ (d: beam width, Φ: full angle of divergence, both defined via 86.5% power content) in the x- (width) and the y-direction (height) for a pulsed Nd:YAG slab laser system with one oscillator slab and two amplifier slabs of dimensions 7x26x179mm^3. a) unstable resonator with VRM having profile radii of 2mm and 7mm in the x- and y-direction, respectively; b) stable resonator with length 550mm, flat output coupler and 2m concave HR mirror. The schematic shows the set-up with the unstable resonator. Total pump energy: 3,400J; pulse length: 4ms. Data are shown for one (osc.), two (osc./amp.) and three slabs (osc./amp./amp.) [3.165] (© OSA 1993).

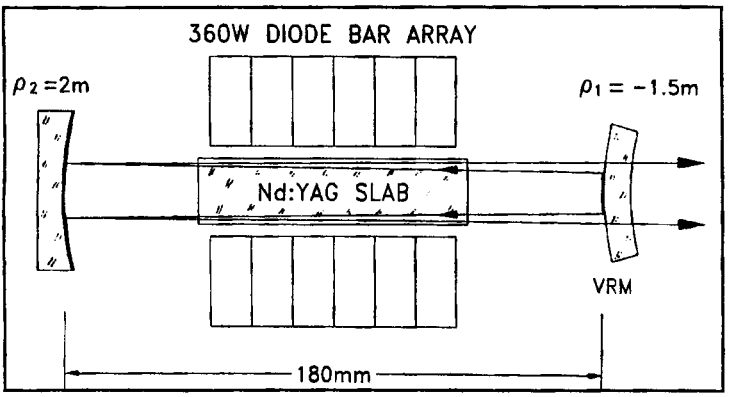

Fig.7.54 Top view of a stable-unstable resonator used in a diode-pumped thin Nd:YAG slab laser. A cylindrical output coupler substrate with a variable reflectivity mirror (VRM) and a spherical high reflector are used to realize a positive branch unstable resonator with magnification M=1.26 in the horizontal direction and a stable resonator in the perpendicular direction [3.176] (© OSA

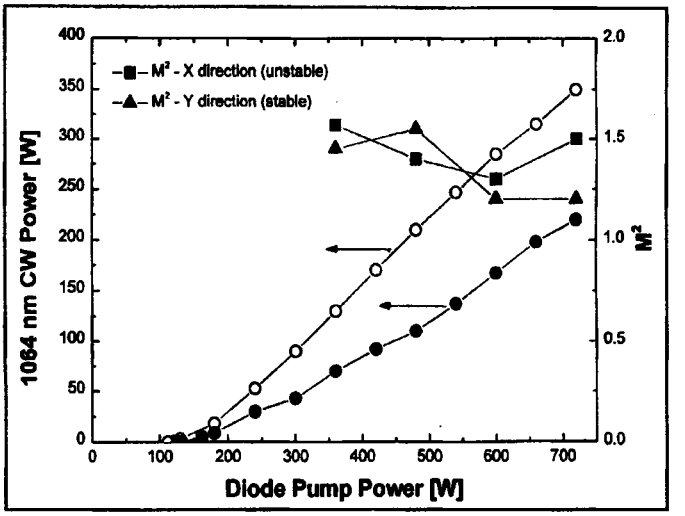

Fig.7.55 Measured output power of the slab laser shown in Fig. 7.54, with a short, stable resonator (open dots) and with the stable-unstable resonator with VRM (filled dots). For the latter resonator, the measured M^2 values in the x-direction (unstable) and the y-direction (stable) are shown as well [3.176] (© OSA 2002).

The lower efficiency of unstable resonators is caused by diffraction losses generated by the edges of the active medium in combination with a lower mode volume. As will be discussed in Chapter 11, unstable resonators generally provide only 70-80% of the extraction efficiency attainable with short stable resonators. The reflectivity profile of the VRM is of lower importance for the beam quality, but it considerably affects the near field distribution and the beam propagation. This is shown in Fig. 7.56 in which measured near field and far field intensity distributions for different VRMs with equal profile radii are compared.

If a flat topped intensity distribution in the near field is required (e.g. for efficient filling of amplifier stages), the center reflectivity and the reflectivity profile can be used as design parameters. In order to attain optimum filling of the active medium by the laser mode an optimization of the reflectivity profile is required. Since the adaptation of the beam width to the width of the active medium is easier to accomplish if the mode exhibits steep slopes, super-Gaussian profiles with high index n provide better means to maximize the output power. For an unstable resonator with a Gaussian VRM, a complete filling of the active medium will generate side lobes in the far field. However, for super-Gaussian profiles with $n>2$, the super-Gaussian field distributions at the output coupler are not eigensolutions of the paraxial wave-equation. The intensity distributions inside the resonator, therefore, will change when the field propagates inside the resonator. This may result in ripples and hot spots. The same statement holds for the field transmitted through the VRM. Depending on the type of application and the damage threshold of the optical components used, the beam propagation has also to be considered when the reflectance profile is chosen [3. 159].

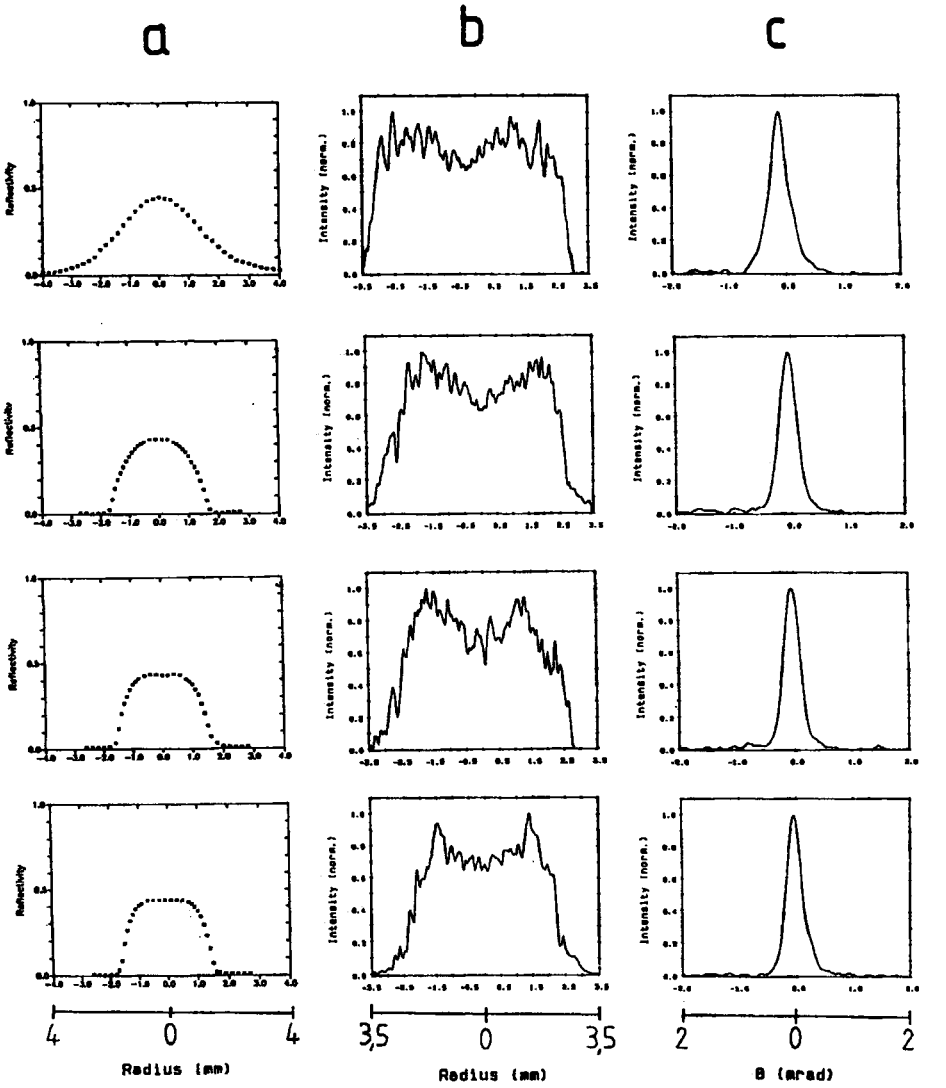

Fig. 7.56 Measured reflectivity profiles of the VRM (a), near field intensity distributions (b), and far field intensity distributions (c) for a confocal unstable resonator with magnification $M=1.5$ (pulsed Nd:YAG rod laser, $\lambda=1.064\mu m$, single shot operation).